Alma Mater Studiorum · Università di Bologna
SCHOOL OF ENGINEERING AND ARCHITECTURE
Forli Campus

SECOND CYCLE MASTER'S DEGREE IN
INGEGNERIA AEROSPAZIALE/AEROSPACE ENGINEERING
class LM-20

MODELING AND OPTIMAL FLIGHT CONTROL OF A FOILING DINGHY

CANDIDATE:
Marco Francioni

MATRICOLA $n°$:
0000754747

SUPERVISOR:
Paolo Castaldi

ASSISTANT SUPERVISOR:
Matteo Zanzi

Academic Year 2020/2021

To my mother

Contents

1 Boat description **14**

2 Model **19**
2.1 Frames of reference 20
2.2 Physics 23
2.3 Sail Forces 27
2.4 Mass Forces 29
2.5 Buoyancy Forces 30
2.6 Foil Forces 31
2.7 State Vector & Input Vector 35
2.8 Environment 38

3 Reduced steady state model for Trim **41**

4 Optimal Control Problem **44**
4.1 Different Approach 50
4.2 Modes of control 52
4.3 Weighting choice 56

5 Gain scheduling for Tack/Jibe maneuver **60**

6 Simulation **66**
6.1 Wave response/rejection 67
6.2 Tack/Jibe simulation 70
6.3 Sensitivity 81
6.3.1 Reduced Integral Iesults 83

6.3.2 Complete Integral Results 84
6.3.3 Comparison 84
6.4 Performance Tricks: how to exploit physics to increase performance 85

List of Figures

1.1 Body 3D 15
1.2 Double Crew Dinghy 17
1.3 Single Handed Foiler 17
1.4 Rigid sail drone 18
1.5 Back View 18

2.1 Wind FoR 22
2.2 Sail Forces 24
2.3 Righting Moment 25
2.4 Point Of Sail 26
2.5 Foil force 31
2.6 Main foil polar 32
2.7 Main foil interpolation scheme 33
2.8 6DOF kinematics 35
2.9 Wind 38
2.10 Wave 39

4.1 Proportional integrator LQ OCP 48
4.2 Modified Proportional integrator LQ OCP 50

5.1 Tack Sail Force oscillation 61
5.2 Sign Vs $\tan^{-1}$ 62
5.3 Scheduler 64

6.1 Wave response 68
6.2 Tack maneuver in calm sea 71
6.3 Tack maneuver in 0.2m waves 72

6.4 Tack maneuver in 0.6m waves 73
6.5 Two well performed opposite tacks in the same environment 74
6.6 Well performed tack followed by a slower one 75
6.7 Well performed tack followed by a faster one 75
6.8 Two identical tacks performed in different TWS . . 76
6.9 Two well performed Jibes 78
6.10 Two tacks in 0.2m wave in "Forced Fast" mode . . 79
6.11 Two tacks in 0.2m wave in "Standard" mode 80
6.12 Flight in marginally conditions 85

List of Acronyms

- **DoF** Degrees of freedom
- **FoR** Frame of Reference
- **NED** Nord East Down FoR
- **HDG** Heading(ψ)
- λ latitide
- φ longitude
- **TWV** True Wind Vector: Wind vector as seen by a stationary observer.
- **AWV** Apparent Wind Vector: Wind vector as seen by a moving observer
- **TWA** True Wind Angle: Angle between the wind direction and the horizontal projection of the X_b axis
- **AWA** Apparent Wind Angle
- **TWS** True Wind Speed
- **AWS** Apparent Wind Speed
- **VMG** Velocity Made Good X_e component of the boat speed
- **AoA** Angle of Attack

- $\mathbf{C}_l$ Lift coefficient
- $\mathbf{C}_{d0}$ Parassite drag coefficient
- $\mathbf{C}_m$ Moment coefficient
- **L** lift
- **D** drag
- $*_{\mathbf{sx}}$ relative to the left half main foil
- $*_{\mathbf{dx}}$ relative to the right half main foil
- $*_{\mathbf{r}}$ relative to the rudder
- $*_{\mathbf{t}}$ relative to the t foil
- **CG** center of gravity or body FoR origin
- $\overline{g}$ gravity vector
- $\overline{\tau}$ applied torque
- $*_b$ Generic quantity in Body FoR
- $*_e$ Generic quantity in NED FoR
- $*_a w$ Generic quantity in Wind FoR item $*_w$ Generic quantity in Water FoR
- $*_{\mathbf{v}}$ Generic quantity in vertical FoR
- $*_s$ Generic quantity relative to set-point
- $*_{[ref]}$ Generic quantity used for reference by the closed loop
- $*^{\mathbf{f}}$ Generic integrated quantity
- **x** state vector

- **u** control vector
- ϕ heeling angle
- θ pitch angle
- ψ 3^{rd} component of the **x** vector can be defined ad HDG or TWA in various instances
- $\mathbf{DCM}_a b$ Direction cosine matrix such that $*_a = DCM_a b *_b$
- $\overline{X}$ 3D position in body axis
- $\delta_{\mathbf{r}}$ rudder deflection
- **LTI** Linear time invariant
- **LQ** liner quadratic
- **OCP** optimal control problem
- **SISO** single input single output
- **MIMO** multiple input multiple output
- **PI** proportional integrator
- **ARE** Algebraic Riccati Equation

Abstract

This Master Thesis illustrates the physics behind the mathematical model of a foiling sailboat to be used in a model-based autopilot architecture, and the multiple frames of references needed for an exhaustive force description. Using the modeled foiling boat, we performed the non trivial task of finding meaningful trim setpoints, which were then used throughout the simulations. We applied Optimal Control theories to achieve stability and control of a foiling dinghy with movable crew at different trim settings and various environmental parameters, such as wind speed and sea state, both stationary and time varying. We developed a prototype of a gain scheduler for the closed loop to perform tack and jibes maneuvers in multiple environments, and compared the stability and parameters sensitivity of different closed feedback loop architectures, both in straight line and maneuvering performance. The maneuvering performances were established with extensive ad-hoc simulations to properly characterize the architectures behavior, while the straight line response and parameter variation sensitivity were determined through Monte Carlo simulations. At the end of this paperwork the two best performing closed loop architectures proposed were compared to determine which one would be the more promising for a practical application.

Introduction

In the last years, the world of racing dinghies and high performance sailboats has seen a growing interest in foiling boats due to improvements in construction materials and technical know how. Foiling dinghies are renown for their instability and difficulty of usage while providing incomparable performances. The aim of this thesis is to study a feasible control loop architecture to achieve a stable and controlled flight in changing environmental conditions. This led to the challenging task of filling the niche of model-based foiling sailboat autopilot, which, up to the beginning of this work, was scarce of scientific literature. To fulfill this goal, an important feature is the ability to perform maneuvers such as tacks and jibes, which is a non trivial accomplishment due to the continuous shifting of the sailing condition from one tack to the other, while maintaining a stable flight through a range of TWAs where the sail cannot provide enough thrust.

In this paperwork we will address:

- Boat description
- Sailboat Physics insight and Mathematical Model
- Trim Condition
- Optimal Control Architectures
- Tack/Jibe Maneuver
- Simulation Results Analysis

In the first chapter we will look at the design choices to understand the geometrical features of the selected vehicle.

In the second chapter we will discuss how the forces and moments are generated by the interaction of the sailboat with the different environments to which the dinghy is subjected.

In the third chapter we will focus on how a trimming point can be found.

In the fourth chapter different approaches to the control loop architecture will be proposed and discussed.

In the fifth chapter we will tackle the challenges of changing tack through maneuvers and we will discuss the solutions found.

In the sixth chapter we will comment the simulations results and compare the different architecture performances.

Chapter 1

Boat description

Lenght	4.2 m
Width	2.1 m
Boat Weight	130 kg
Movable Weight	140 kg
Sail Area	$18m^2$
Main Foil Area	$1.5m^2$

The boat is a 14" dinghy with a crew of two. The hull purpose is only to provide buoyancy and stability at null speed prior to take-off and minimization of aerodynamic drag once foil-borne. Its shape will be not discussed in this paperwork [13].

The movable weight (Crew Mass) is an indicative estimation for two average sized 70kg fully rigged sailors, its position is offset from the center-line to provide righting moment while hanging on trapeze. The crew is supposed to hike on the harness standing in an almost horizontal fashion from the side of the platform, its center of mass is estimated to be 1m outboard of the trampoline limit fixed by R3 class rules [12]. The main feature of this boat is a hydrofoil, which is connected to the hull by two airfoil shaped struts and provides lift in order to reduce overall wet surface once foiling. The main foil is equipped with two flaps independently actuated. The leeward half section will provide most of the lift,

while the upwind portion can be used to provide lift or down force. At slow speeds, the upwind semi foil helps to lift the boat out of the water by providing a larger C_l through out the whole main foil. Once high speed are reached the leeward semi-foil is capable to provide enough lift by itself and the windward flap section can switch to a down-force configuration(negative flap angle) to provide righting moment when the weight and displacement of the crew will not be enough to keep a fixed heel angle at increased AWS. Being the compression load on the struts proportional to V_b^2, there is not an upper bound. Therefore, for a practical application, some kind of limit must be ensured to guarantee the structural integrity.

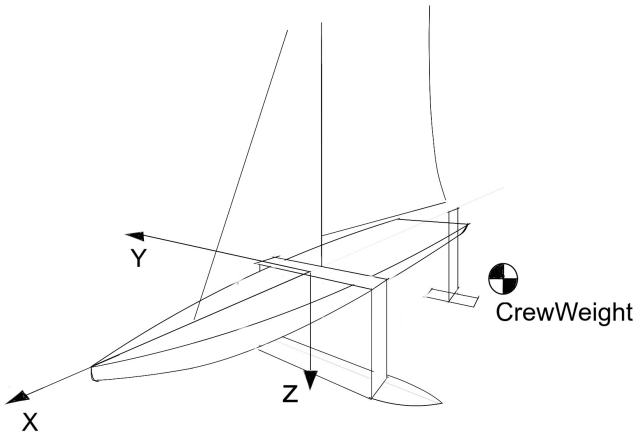

Figure 1.1: Body 3D

A real concern with a fully immersed foil is the lack of heave stability and neutral roll stability. The main purpose of the main-foil flaps with its control loop is to have stability on both degrees of freedom while allowing the crew to be focused on sail. The roll instability is a major concern in double handed sailboats because

any correction made by the movement of both crew members can badly interact on a sensitive parameter such as ϕ angle. As a comparison if anyone can stand on a single foot, doing the same with another person on the back is more of an acrobat set of skills than an athletic goal. The same can be applied on Foilers, a single crew can achieve roll equilibrium near the optimal ϕ by itself, but on double handed sailboats crew weight movement will result in Pilot Induced Oscillations or worst, a capsize.

The rudder at the stern mounts an elevator at its tip to provide pitch control and allows the weight of the crew to be shifted back and forth along the longitudinal axis with minor effect on the attitude of the boat, although a sweet spot for performance and stability can be found.
The rig started as a classical jib-main sail plan with an additional hoistable gennaker (25 m^2) for low wind broad reach sailing and was controlled by the usual set of sheets. But, with an eye on automation, it has been changed to a rigid wing actuated by a trim-tab on the trailing edge of the sail to have a direct control of the AoA of the sail. This configuration reduces the already intense workload of the computing hardware and avoids the modeling the slack of the sheets, resulting in a more linear and stable configuration for the control loop in a wide range of TWAs, which decouples the sail input with respect to the AWA.

$$\mathbf{B} = \aleph(\mathbf{x}, \mathbf{u}) \rightarrow \mathbf{B} = \aleph(\mathbf{x}) \circ \mathcal{L}(\mathbf{u}) \tag{1.1}$$

it seems a minor improvement but as we will discuss later the already marginal numerical stability is largely improved. The new configuration changes the sail plain response to an angular shift in wind direction. In fact, a "lift" on a classical configuration will increase the AoA of the sail, increasing heeling moment, while in our AoA direct configuration, the same "lift" will cause a sail rotation along with the Apparent Wind frame of reference, resulting in a reduction of heeling moment and introducing a down pitching moment due to the increased thrust.

Figure 1.2: Double Crew Dinghy

Figure 1.3: Single handed Foiler

Figure 1.4: Rigid sail drone

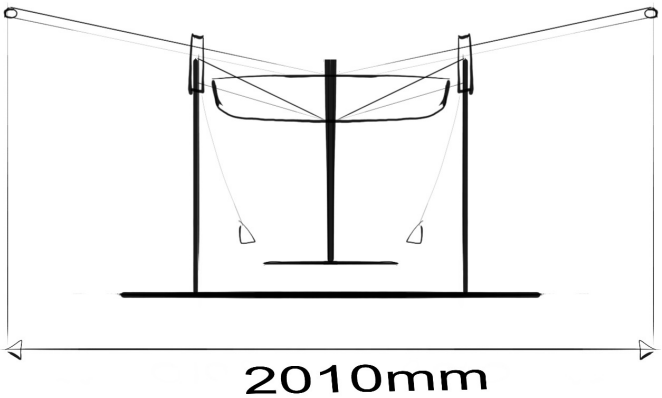

Figure 1.5: back view

Chapter 2

Model

The simulator has been built from the ground up exploiting the 6dof custom variable mass block from the Simulink, which receives force and moments expressed in body frame and gives the body kinematics[5] [6].
matlab referenxce
The forces acting on the vessel come from different environments, each one with its own frame of reference. As an example gravity forces are always aliened with NED (z) [1][2]axis.

To simplify true wind speed as well, TWV is aligned, by default, to the same frame of reference flowing horizontally from North to South with no wind profile due to marine boundary layer, even though there are no issues other than keeping track of the sign while adding non north component of the wind (on the east-west axis) or wind rotations $\mathbf{R}_{(Z_e)}$ to simulate gust and wind variation. Although possible to add a vertical gust Z_e, it has no physical meaning since at sea level on the sail-scale a vertical gust will be damped by the wall effect of the sea[9]. Differently from other vehicles, the sailboat propulsion comes from an external source: the interaction between wind and water. The two frames, depending on the attitude of the boat, can have different orientations that cannot be neglected. An extensive discussion on frame of reference description will follow in the next sections.

2.1 Frames of reference

The rotation between **NED** to Body is defined by the Euler angles $\phi\ \theta\ \psi$[1].

$$\mathbf{v}_b = \mathbf{DCM}_{be}\mathbf{v}_e \tag{2.1}$$

$$\mathbf{DCM}_{be} = \mathbf{R}_\phi\mathbf{R}_\theta\mathbf{R}_\psi \tag{2.2}$$

$$\mathbf{R}_\psi = \begin{bmatrix} cos(\psi) & sin(\psi) & 0 \\ -sin(\psi) & cos(\psi) & 0 \\ 0 & 0 & 1 \end{bmatrix} \tag{2.3}$$

$$\mathbf{R}_\theta = \begin{bmatrix} cos(\theta) & 0 & -sin(\theta) \\ 0 & 1 & 0 \\ sin(\theta) & 0 & cos(\theta) \end{bmatrix} \tag{2.4}$$

$$\mathbf{R}_\phi = \begin{bmatrix} 1 & 0 & 0 \\ 0 & cos(\phi) & sin(\phi) \\ 0 & -sin(\phi) & cos(\phi) \end{bmatrix} \tag{2.5}$$

where the inverse rotation is defined as

$$\mathbf{DCM}eb = \mathbf{DCM}be^{-1} = \mathbf{R}_\psi^T\mathbf{R}_\theta^T\mathbf{R}_\phi^T \tag{2.6}$$

The apparent wind is defined as the vectorial sum of the True wind vector and the velocity vector.

$$\mathbf{AWV}_b = \mathbf{TWV}_b + (\mathbf{V}_b + \overline{X}_{sail} \times \omega) \tag{2.7}$$

The AWA which has relevance on the sail/wind interaction is defined as

$$AWA = arctan(-\mathbf{AWV}_{b_y}/\mathbf{AWV}_{b_x}) \tag{2.8}$$

the Apparent wind angle will define the rotation matrix for the sail force

$$\mathbf{R}_{bAWA} = \begin{bmatrix} cos(AWA) & sin(AWA) & 0 \\ -sin(AWA) & cos(AWA) & 0 \\ 0 & 0 & 1 \end{bmatrix} \tag{2.9}$$

Assuming stationary water, we can define the water angle α, β as:

$$\alpha = arctan(\mathbf{V}_{b_z}/\mathbf{V}_{b_x}) \tag{2.10}$$

$$\beta = arctan(\mathbf{V}_{b_y}/\mathbf{V}_{b_x}) \tag{2.11}$$

The forces and moment produced by the foils are aligned with the water reference frame, therefore, to compute such vectors in body coordinate

$$\mathbf{V}_b = \mathbf{DCM}_{bw}\mathbf{V}_w \tag{2.12}$$

$$\mathbf{DCM}_{bw} = \mathbf{R}_\alpha \mathbf{R}_\beta \tag{2.13}$$

$$\mathbf{R}_\alpha = \begin{bmatrix} cos(\alpha) & 0 & -sin(\alpha) \\ 0 & 1 & 0 \\ sin(\alpha) & 0 & cos(\alpha) \end{bmatrix} \tag{2.14}$$

$$\mathbf{R}_\beta = \begin{bmatrix} cos(\beta) & -sin(\beta) & 0 \\ sin(\beta) & cos(\beta) & 0 \\ 0 & 0 & 1 \end{bmatrix} \tag{2.15}$$

The wind reference frame is similar to **NED** but needs to be aligned with the wind direction. From the boat point of view, what can be seen is the apparent wind

$$\mathbf{TWV}_b = \mathbf{AWV}_b - \mathbf{V}_b \tag{2.16}$$

To evaluate the TWA we need to generate a local vertical Frame of Reference aligned with the horizontal projection of x_b

$$\mathbf{DCM}_{vb} = \mathbf{R}_\theta^T \mathbf{R}_\phi^T \tag{2.17}$$

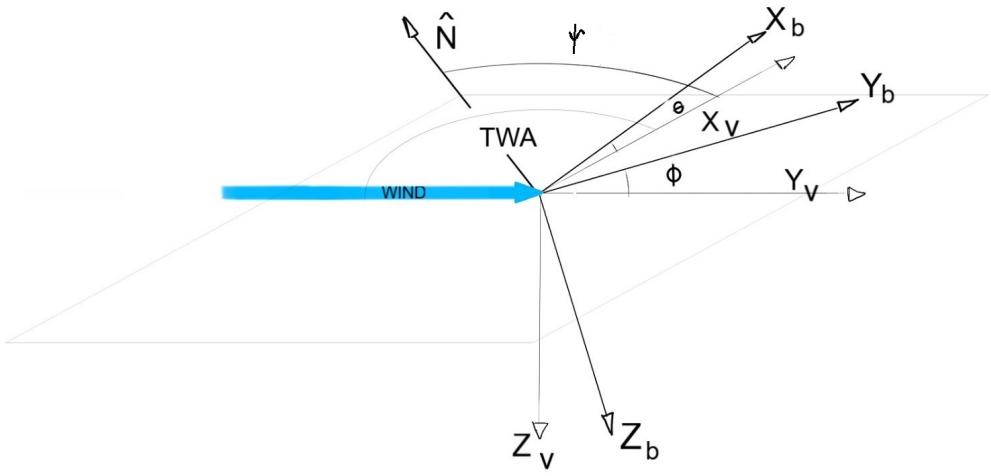

Figure 2.1: Wind FoR

now the TWA can be found as

$$TWA = arctan(-\mathbf{TWV}_{v_y}/\mathbf{TWV}_{v_x}) \tag{2.18}$$

to have positive TWA when the boat is on the left tack.

2.2 Physics

There is not a skewer vehicle than a sailing boat. The romantic image of a sailing yacht cruising in the sunset is actually a slanted plethora of forces in perfect balance acting in different directions with no means of symmetry.

The sail can be seen as a wing subjected to the apparent wind, which is the vectorial sum of the True wind, the one felt by a stationary observer, and the relative wind produced by the boat motion. We know that the force produced by a finite wing can be computed in two components one generally called Lift, normal to the apparent wind direction and to the wing spar (mast), and one parallel to the wind direction generally called drag[1][2].

$$Lift_{sail} = \frac{1}{2}\rho_{air} C_{l_{sail}} AWS^2 sign(AWA) \tag{2.19}$$

$$Drag_{sail} = \frac{1}{2}\rho_{air} C_{d_{sail}} AWS^2 \tag{2.20}$$

The resultant must be rotated by AWA into body FoR and can be split into longitudinal component (thrust) and a sideways force(leeway), as we can see in 2.2 The efficiency of the sail actually improves the close-hauled performance allowing to have the same thrust at smaller AWA. The sideways component is usually balanced by the dagger board lift. In this case, the windward heeling allows the weight to have a component that acts against the leeway force (the vertical portion in NED) while the main contribute to counteract the leeway force is given by the foils lift. Being the hull tilted by a specific amount in NED coordinates we can recognize a vertical component of the main-foil lift that counteracts the gravity force and an horizontal component against leeway. An important aspect of the equilibrium that must be noticed is the position of the application points of the already mentioned forces. As we can see from the 2.3 we have the sail force high above deck the leeway on a port tack will induce a

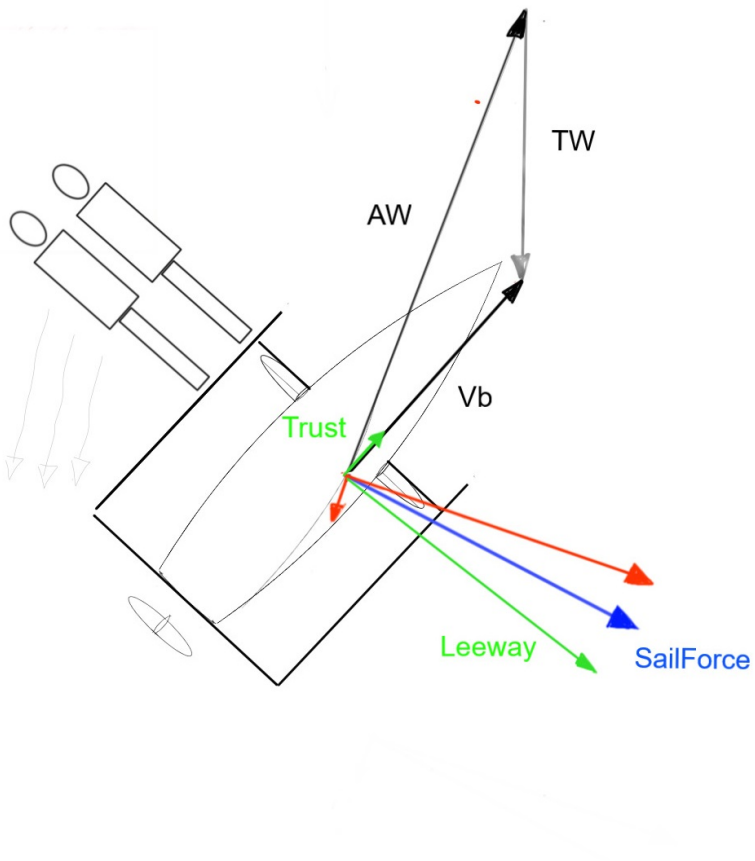

Figure 2.2: Sail Forces

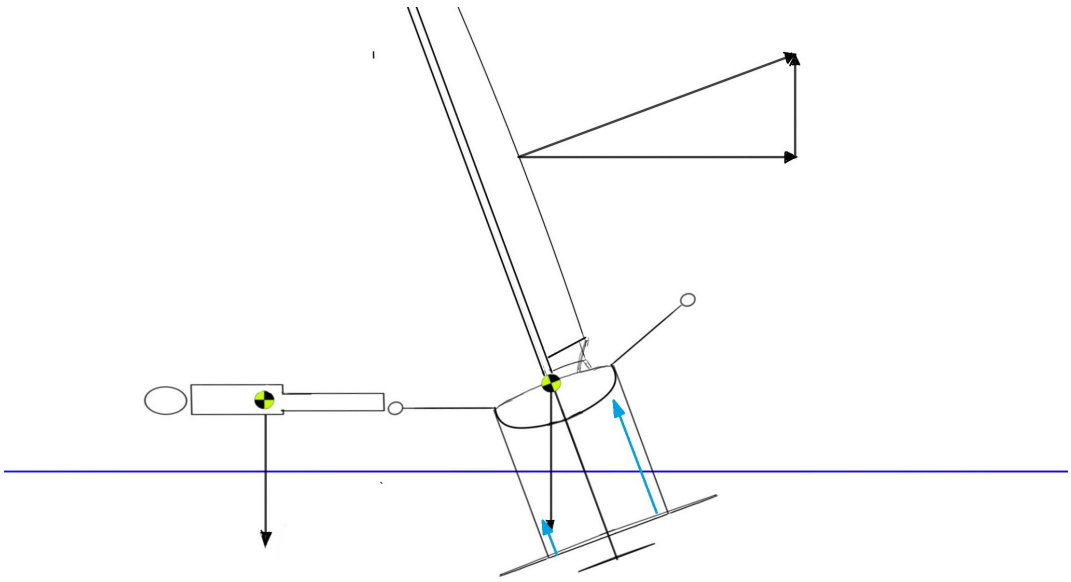

Figure 2.3: Righting Moment

positive roll while the offset weight of the crew will balance it, aided also by a different amount of flap deflection on the main foils. On the pitch axis the situation is fairly similar, although the components in place are lower. Therefore, it is much easier to balance the pitching moment thanks to the T-foil on the rudder. The righting moment applied from the crew position and the total weight can be considered as constant even though the crew is allowed to move around the platform. The position far outboard achieves the maximum righting moment, therefore, at maximum performance, it can be considered fixed at its maximum displacement in any trim (non maneuvering) condition. Knowing the sail center of pressure, the weights and the allowed Crew position an optimal heeling(ϕ) can be evaluated by solving the system:

$$\mathbf{F}_{sail_y} cos(\phi) = -(L_{dx} + L_{sx}) sin(\phi) \quad (2.21)$$
$$(L_{dx} + L_{sx}) cos(\phi) - \mathbf{F}_{sail_y} sin(\phi) = -(M_{crew} + M_{boat}) g \quad (2.22)$$
$$M_{crew}(Y_{crew}) cos(\phi) - Z_{crew} sin(\phi)) g = -\mathbf{F}_{sail_y} Z_{sail} \quad (2.23)$$

Neglecting Rudder force and assuming the β angle to be null, the optimal ϕ for this boat is around $\simeq -17°$.

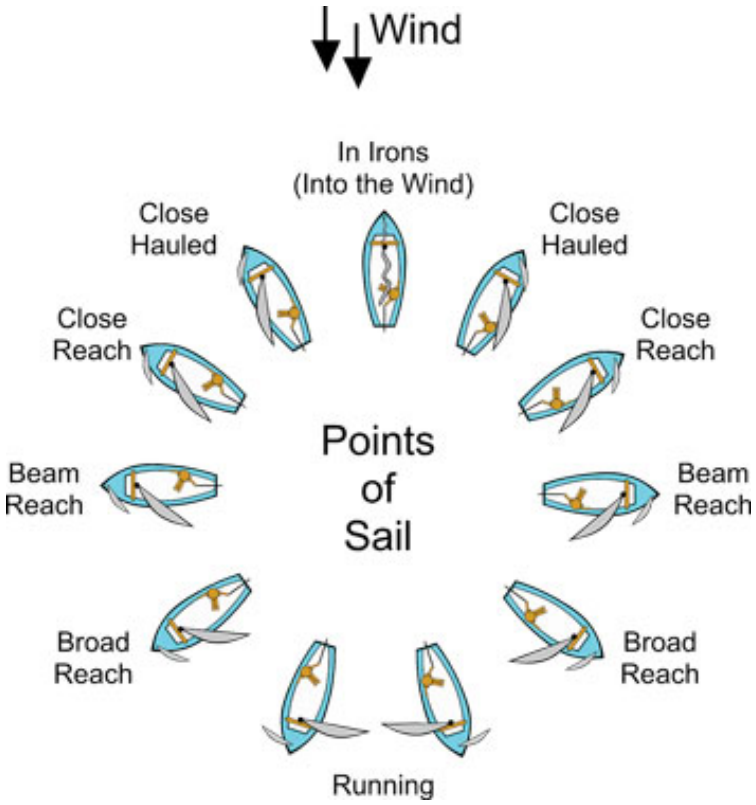

Figure 2.4: Point of Sail

2.3 Sail Forces

As we have seen, the windage of the boat does not feel the True Wind but the Apparent one that is created by the vectorial sum of wind and boat velocity. The sail's center of pressure is far away from the CG of the boat, therefore, any rotation affects the actual boat velocity components. The handiness of a NED defined wind means that it can be simply added to the V_e as X_e and Y_e components as seen in Fig2.9. The AWVector is then rotated in body frame to compute its X_b and Y_b components to determine the Apparent Wind Angle while the Z_b component is discarded. Being parallel to mast, its effect on the sail will be analogous to the sweep of a wing, therefore negligible. Discarding the third component simulates also the reduction of projected sail area due to heel Angle(ϕ) with the adjoint benefit of a consistent definition of AWA regarding the sail airfoil. The sail is defined as a finite wing with lift, drag and moments. It is to be noticed that the center of lift is high above the deck and produces an heeling (Rolling) moment to leeway and a thrust-related pitching down moment. As already mentioned, the modeling of the sail actuation refers to the AoA while classic sailboats can only control the sail orientation with respect of the hull center-line by means of sheets and running rigging. The different emerging dynamics have to be taken into consideration when different setups are employed, meaning that a straight forward carry-trough of the closed loop cannot be applied without a proper study. Sailors can continuously exploit the flexibility of the sail and change twist, camber and camber position to improve performance. This feature is well above this model and therefore has been neglected, even though the sail centroid position can be changed by workspace variable in accordance with the rigid wing-sail model.

The hull and the crew have a fictional surface area and a Cd of 0.5, the hull increases its projected area proportional to its length with a broader AWA. Aligning the lift and drag with the proper AW frame is essential since the boat standing still and pointing south will have a possible AWA range within $\pm 180°$. Once force and moments are generated they are rotated in body frame to be consistently sent to the 6 DoF block.

$$L_{sail} = \frac{1}{2}\rho_{air} AWS^2 S_{sail} C_{l_{sail}} \tag{2.24}$$

$$C_{l_{sail}} = C_{l\alpha_{sail}}\alpha + C_{l_0} \tag{2.25}$$

$$D_{sail} = \frac{1}{2}\rho_{air} AWS^2 S_{sail}[C_{d_0} + \frac{C_{l_{sail}}^2}{AR_{sail}\pi e_{sail}}] \tag{2.26}$$

$$F_{sail_{x_b}} = (L_{sail}) * sin(AWA) - (D_{sail}) * cos(AWA) \tag{2.27}$$

$$F_{sail_{y_b}} = (L_{sail}) * cos(AWA) + (D_{sail}) * sin(AWA) \tag{2.28}$$

with the sail force, it is useful to introduce the equation for Crew-hull drag, since it is generated in the same Frame of Reference. Therefore, it is subjected by the same rotation.

$$D_{hull_b} = \frac{1}{2}\rho_{air} AWS\,^2 C_{d_h} h_h (l_h \| s(AWA) \| + (b_h + 1.8) \| c(AWA) \|) \tag{2.29}$$

2.4 Mass Forces

This block needs to know the position of the crew on the boat in x and y while z=f(y). The body frame of reference remains fixed in position while the Crew mass moves around. Its position affects the inertial ellipsoid of the vehicle evaluated by the block itself. The abrupt movement of the crew will generate an applied force through the boat simulated as an adjoint (-)acceleration on top of the gravity vector for the crew only[7]. The boat acceleration will generate inertial moments due to the distance from crew center of mass position and center of mass (fixed) of the boat. The block takes care of it having all the necessary information. By the way, since the crew mass is roughly half of the total mass, keeping a moving crew will badly affect the numerical stability of the simulation. Therefore, once the crew settles on a trim point position, it is kept fixed in place with all the other controls acting to maintain equilibrium. The only situations in which the crew is allowed to move are during tack and jibe maneuvers. The boat CG translatory acceleration generates an inertial torque due to crew CG position, while rotatory acceleration and centrifugal forces have been neglected due to slow rotation rate of the vessel in simulated trim condition.

$$\mathbf{F}_{m_b} = \mathbf{DCM}_{be}(M_{crew} + M_{boat})\overline{g} \tag{2.30}$$

$$\overline{\tau}_b = M_{crew} \cdot \overline{X_c} \times (\mathbf{DCM}_{be}(\overline{g}_e) - \dot{\overline{V_b}}) - M_{crew}\ddot{\overline{X_c}} \tag{2.31}$$

2.5 Buoyancy Forces

The hull volume is box shaped. This block gives the buoyancy platform to allow standing start of the simulation with a drag fixed to $0.1 * Buoyancy$ aligned with X_b therefore it is not meant to study the proper take-off dynamics. During normal operation the hull should never touch the water, the presence of some kind of drag is necessary to slow down the boat once the hull touches the water during a simulation. A proper take-off evaluation has been conducted during the preliminary design of the project[4] to assure the capability of taking off. However, since its complex dynamics are dependent on wave and spray produced by the hull, they affect a small percentage of the simulation time and can be neglected. The adjoint benefit of such model is an exaggerated speed reduction in "capsized" situation that allows to detect such condition by simply evaluating boat speed. The modularity of the model allows further development with little effort on this regard.

$$\mathbf{F}_{buoyancy_e} = -\rho_{water} * l_h * b_h * Hulldraft * \overline{g} \tag{2.32}$$

$$\mathbf{F}_{buoyancy_b} = \mathbf{DCM}_{be}\mathbf{F}_{buoyancy_e} \tag{2.33}$$

2.6 Foil Forces

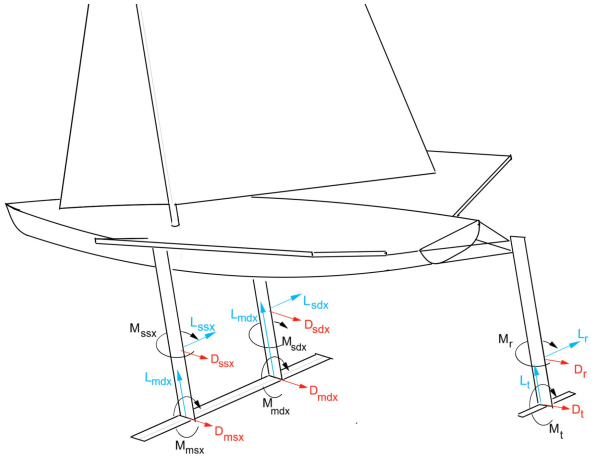

Figure 2.5: Foil force

The foil architecture concerns 6 elements: 2 vertical struts, left and right halves of the main-wing, rudder and elevator. Each element has its own specifically designed airfoil with polars generated on Xfoil linearly interpolated between op-points. Special care was given to the main-wing , since it has a flap that is an active control for the heave (vertical) stability and roll. Two sets of polars for the left and right halves of the flap are evaluated.

These polars have two variables: angle of flap deflection and angle of attack, the resulting 3D arrays are then interpolated. At each time the main-foil will have a defined set of coefficient $\mathcal{C}(\alpha_\star, f_\star)$. We can evaluate $\mathcal{C}(\alpha_\star, f_\star)$ by interpolating the closest op-points where the polar is evaluated by Xfoil:

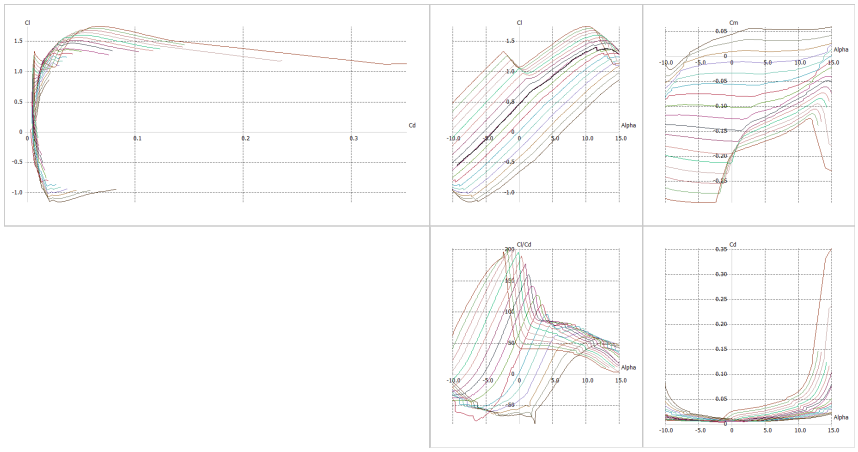

Figure 2.6: Main foil polar

We can define α_- & α_+ as the closest evaluated AoAs to $\alpha_\bigstar$ such that $\alpha_- \leq \alpha_\bigstar \leq \alpha_+$ and similarly $f_- \leq f_\bigstar \leq f_+$. We can evaluate the relative distance of the actual operating point $\bigstar$ inside the polar step with respect to the evaluated op-points as $\frac{\delta\alpha}{\Delta\alpha}$ and $\frac{\delta f}{\Delta f}$ where $\Delta\alpha$ and Δf are the polar evaluation steps and $\delta\alpha$ and δf are the distances of $\bigstar$ from the α_-, f_- as shown in Fig2.7. The coefficient of the other surfaces are evaluated in a similar fashion without any flap deflection.

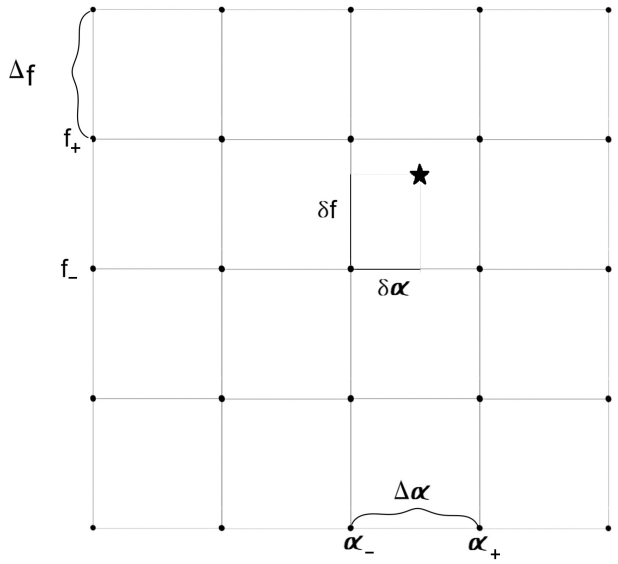

Figure 2.7: Main foil interpolation scheme

$$\mathcal{C}(\alpha_\bigstar, f_\bigstar) = \frac{\delta\alpha}{\Delta\alpha}\frac{\delta f}{\Delta f}\mathcal{C}(\alpha_+, f_+) + (1 - \frac{\delta\alpha}{\Delta\alpha})\frac{\delta f}{\Delta f}\mathcal{C}(\alpha_-, f_+) + \\ + \frac{\delta\alpha}{\Delta\alpha}(1 - \frac{\delta f}{\Delta f})\mathcal{C}(\alpha_+, f_-) + (1 - \frac{\delta\alpha}{\Delta\alpha})(1 - \frac{\delta f}{\Delta f})\mathcal{C}(\alpha_-, f_-) \tag{2.34}$$

Each fully submerged element has an assigned position relative to the boat reduction center while the surface piercing elements are considered solely for their wetted surface, with varying aspect ratio and the centroid positions sliding to the tip of each element while the vessel emerges. With the emerged length

$$H = \frac{-z_e + x\ sin(\theta) - y\ sin(\phi)}{cos(\phi)cos(\theta)} \tag{2.35}$$

$$\overline{X}_{SurfacePiercing} = [x, y, \frac{H + Draft}{2}] \tag{2.36}$$

The AoA is computed taking care of water velocity and rotational rates evaluated at the centroid positions.

$$\mathbf{V}_{local} = \mathbf{V}_b - \overline{X}_{element} \times \omega_b \tag{2.37}$$

Force and moment are evaluated in water axis, although alpha and beta are sub one degree for trim condition. The water is considered to be stationary since there are no current gusts in open water and the tidal period is many order of magnitude larger than the timescale of this simulation. Therefore, it can be considered as a static quantity that will not affect the dynamics. It can be modeled as an added horizontal movement in the navigation problem. Vertical and horizontal motion related to sea state is modeled as a vertical velocity superposition affecting only the foil force block.

$$Lift = 1/2\rho_{water}SV^2C_l \tag{2.38}$$

$$Drag = 1/2\rho_{water}SV^2(C_{d_0} + C_l^2/\pi ARe) \tag{2.39}$$

Each foil has its own C_l, C_{d_0} evaluated with polars, applied on its centroid to compute torque.

$$\overline{\tau} = \mathbf{r} \times \mathbf{F} \tag{2.40}$$

2.7 State Vector & Input Vector

The State Vector $\mathbf{x}$ is defined as:

$$\mathbf{x} = [\phi, \theta, \psi, p, q, r, u_b, v_b, w_b, z_e] \tag{2.41}$$

With dimension $[rad][rad/s][m/s][m]$

The control vector $\mathbf{u}$ is defined as:

$$\mathbf{u} = [AoA_{sail}, Avg_{flap}, \Delta_{flap}, \delta_t, \delta_r] \tag{2.42}$$

All $\mathbf{u}$ values are expressed in [$^\circ$] The difference in units between $\mathbf{x}, \mathbf{u}$ will affect the weighting of the cost function with the $\mathbf{Q}$ entries relative to the rad values scaled by $180/\pi$

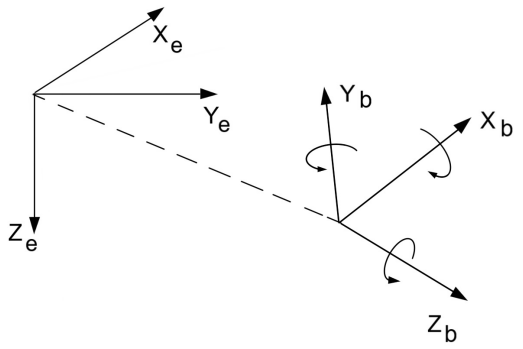

Figure 2.8: 6DOF kinematics

$$\begin{bmatrix} \dot{x} \\ y \\ z \end{bmatrix}_e = \mathbf{DCM}_{eb}(\mathbf{x}) \begin{bmatrix} u \\ v \\ w \end{bmatrix}_b \tag{2.43}$$

$$
\begin{aligned}
&\begin{bmatrix}\dot{u}\\ \dot{v}\\ \dot{w}\end{bmatrix}_b + \begin{bmatrix}p\\ q\\ r\end{bmatrix}_b \times \begin{bmatrix}u\\ v\\ w\end{bmatrix}_b = \\
&= \frac{1}{M_{tot}}\Big[\mathbf{R}_{AWA}(\mathbf{x}, wind)\mathbf{F}_{sail}(\mathbf{x}, \mathbf{u}, wind) + \\
&+ \mathbf{DCM}_{be}(\mathbf{x})\mathbf{F}_m(\mathbf{x}, \mathbf{u}) + \\
&+ \mathbf{DCM}_{bw}(\mathbf{x})\mathbf{F}_{foil}(\mathbf{x}, \mathbf{u}) + \\
&+ \mathbf{DCM}_{be}(\mathbf{x})\mathbf{F}_{buoy}(\mathbf{x})\Big]
\end{aligned}
\tag{2.44}
$$

$$
\begin{aligned}
&\begin{bmatrix}\dot{p}\\ \dot{q}\\ \dot{r}\end{bmatrix}_b + \frac{1}{I}\begin{bmatrix}p\\ q\\ r\end{bmatrix}_b \times \left(I \begin{bmatrix}p\\ q\\ r\end{bmatrix}_b\right) = \\
&= \frac{1}{I}\Big[\mathbf{R}_{AWA}(\mathbf{x}, wind)\overline{\tau}_{sail}(\mathbf{x}, \mathbf{u}, wind) + \\
&+ \mathbf{DCM}_{be}(\mathbf{x})\overline{\tau}_m(\mathbf{x}, \dot{\mathbf{x}}, \mathbf{u}) + \\
&+ \mathbf{DCM}_{bw}(\mathbf{x})\overline{\tau}_{foil}(\mathbf{x}, \mathbf{u})\Big] +
\end{aligned}
\tag{2.45}
$$

with all the torques ($\overline{\tau}$) expressed in body frame

$$
I = \begin{bmatrix} I_{xx} & -I_{xy} & -I_{xz} \\ -I_{yx} & I_{yy} & -I_{yz} \\ -I_{zy} & -I_{zy} & I_{zz} \end{bmatrix} \tag{2.46}
$$

$$\begin{bmatrix} p \\ q \\ r \end{bmatrix}_b = \begin{bmatrix} \dot{\phi} \\ 0 \\ 0 \end{bmatrix}_e + \begin{bmatrix} 1 & 0 & 0 \\ 0 & c(\phi) & s(\phi) \\ 0 & -s(\phi) & c(\phi) \end{bmatrix} \begin{bmatrix} \dot{0} \\ \theta \\ 0 \end{bmatrix}_e + \\ + \begin{bmatrix} 1 & 0 & 0 \\ 0 & c(\phi) & s(\phi) \\ 0 & -s(\phi) & c(\phi) \end{bmatrix} \begin{bmatrix} c(\theta) & 0 & -s(\theta) \\ 0 & 1 & 0 \\ s(\theta) & 0 & c(\theta) \end{bmatrix} \begin{bmatrix} \dot{0} \\ 0 \\ \psi \end{bmatrix}_e \tag{2.47}$$

$$\begin{bmatrix} \dot{\phi} \\ \theta \\ \psi \end{bmatrix} = \begin{bmatrix} 1 & sin(\phi)tan(\theta) & cos(\phi)tan(\theta) \\ 0 & cos(\phi) & -sin(\theta) \\ 0 & sin(\phi)/cos(\theta) & cos(\phi)/cos(\theta) \end{bmatrix} \begin{bmatrix} p \\ q \\ r \end{bmatrix}_b \tag{2.48}$$

It has to be noted that the formulas do not contain any $\dot{m}$ term since the mass is assumed to be constant[5][6].

2.8 Environment

Since the sailboat experiences force through its interaction with environmental quantities some words have to be spent on this regard. As we have already seen the wind is aligned by default with the $\hat{\mathbf{N}}$ in **NED** reference frame. The capability within the model to decouple the wind direction with the **NED** implies that a new frame of reference has to be defined to allow wind rotations.

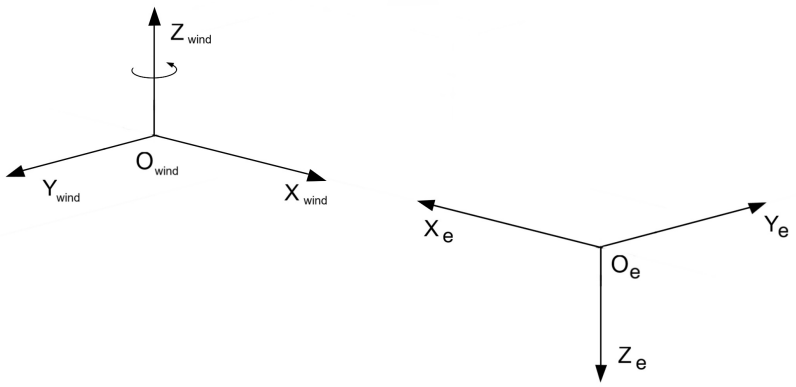

Figure 2.9: Wind

In foiling condition the hull is raised from the water surface by few centimeters (10cm $\rightarrow$ 100 cm). Its interaction with the wave, even if sporadic, can't be neglected while asserting stability and robustness of the control loop during the simulation. The foils are affected by the sea state.The rise and fall of the sea level as a vertical speed component affects the instantaneous water angles.

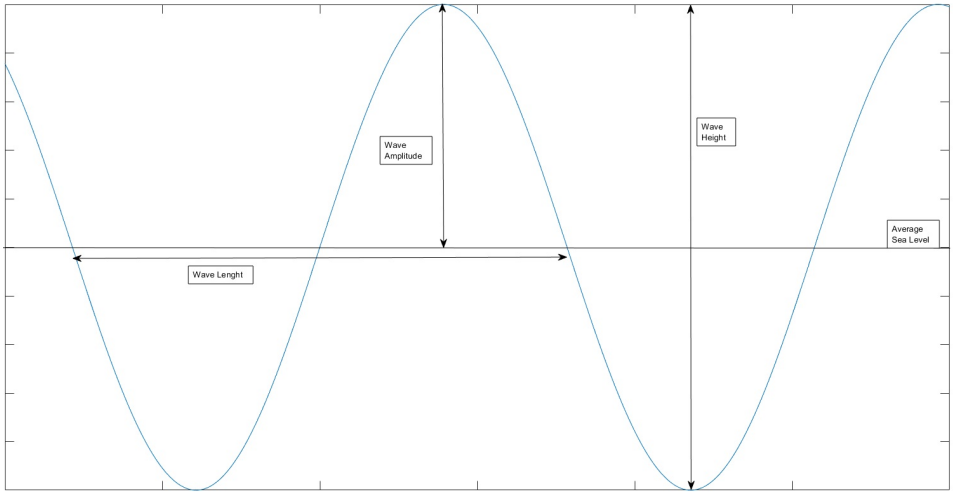

Figure 2.10: Wave Parameters

As we can see from (2.10) the waves are defined as a sinusoid with spatial properties. The sin function in MATLAB, on the other hand, defines its parameters with respect to time. To describe the spatial property Wave Length as a function of time, the period is defined with the ratio $\mathbf{V}_{\mathbf{b_x}}[ref]/WaveLength$. This simplistic model does not take into account the boat velocity variation but is still capable of a meaningful representation of the reality, although changing course will not affect the wave effects on the boat. With the waves defined through wave length(λ_w) and wave height (h_w) we can completely describe the instantaneous water motion around the vehicle[3]. An approximation has been made on where the wave induced water velocity is computed. The effect of the waves is evaluated in a single point 0.7m below the average sea level for all the immersed surfaces.

$$u_w = \Re[sign(\lambda_w)\sqrt{\frac{2\pi g}{|\lambda_w|}}\frac{h_w}{2}e^{-0.7\frac{2\pi}{|\lambda_w|}}e^{i\sqrt{\frac{2\pi g}{|\lambda_w|}}t}] \tag{2.49}$$

$$w_w = \Re[i\sqrt{\frac{2\pi g}{|\lambda_w|}}\frac{h_w}{2}e^{-0.7\frac{2\pi}{|\lambda_w|}}e^{i\sqrt{\frac{2\pi g}{\lambda_w}}t}] \tag{2.50}$$

The if $\lambda_w > 0$ the boat is moving against the wave propagation direction.

An important consideration on the wave definition is where we have to add the wave model. The flat fixed earth implicit in **NED** frame of reference means that we have to superimpose the $\mathbf{Z_e}$ & $\dot{\mathbf{Z}}_\mathbf{e}$ motion of the wave before the Simulink blocks that evaluate the various forces (Buoyancy and Foil blocks). This architecture decouples the foiling height in the state vector with respect to the actual distance of the hull from the water, which is the results of the superposition of the instantaneous wave-defined free surface position and the foiling height.

Chapter 3

Reduced steady state model for Trim

The quest for a meaningful trim point in this boat is somewhat much more complex than the one of a power vehicle. For example, on an airplane, once we are inside the flight envelope, it is very easy to find a first approximation for straight and level flight condition or for a coordinate turn. As we have seen in the chapter of the physics of sailboats, the thrust that sail generates changes with velocity and attitude with respect to the wind, therefore, an approximation of the trim condition must be searched in a non analytical way. To find the trim of the model, an empirical approach has been used with the help of a joystick, a reduced model and some proportional feedback loop later discharged. Being able to find a solution for the full 6 DoF control vector onto the complete model by hand can be very difficult, especially with such an attitude sensitive configuration. Knowing that the heave stability is neutral, a proportional control loop on the flight height/ flap symmetric deflection was installed to achieve a stable flight around a certain nominal height. To reduce the attitude dependence, the moments applied to the body were temporarily disconnected to the "Custom Mass 6 DoF " block to neglect rotations. Having a point mass (3DOF) with fixed attitude (ϕ, θ, ψ) and a constant

TWS,TWD allows us to let the plant find its own trim point velocity wise, while a careful adjusting of the control vector by sliders and knobs of the joystick kept the moments as low as possible. The choice of the non spring-centered axis of the joystick made a very fine tuning of the control vector possible, achieving both force and moments below $10^{-2}N|Nm$ through subsequent run by adding previous $\mathbf{u}$ results and scaling by one order of magnitude the joystick sensitivity. Once a trim condition has been found, the moments are then reconnected to the 6DoF block (back to a 6DoF problem) and a simulation is ran. The results show that for at least 35 seconds the boat remains within the trim point neighborhood before drifting away. These results gave us the possibility to proceed further with the linearization. To find the proper trim the linearization toolbox has been used. At the first try, the plug-in struggled to find any numerical solution and even after a sensible increase of the maximum iteration the trim point was unacceptable, with rotational accelerations over 5 rad/s^2 and control and state vectors substantially different from the ones settled by hand. To find the proper control vector($\mathbf{u}$), the linearization toolbox needs to start near the empirical $\mathbf{u}$ due to the fact that its values differ substantially from the null vector. This insight will be relevant once we will discuss stability and sensitivity of the closed loop system, since the system does not behave well if it stars away from a trim condition $\mathbf{u}$ $\mathbf{x}$ wise.

As result, we have obtained $\mathbf{u}$,$\mathbf{x}$ couples and the $\dot{\mathbf{x}}$ has now entries between 10^{-4} and 10^{-17}.

When the system is around trim conditions, the crew should be quasi static. Since the crew holds a huge percentage of the total mass, having it freely moving on the deck introduces a huge source of non linearity and a hard time for the control loop to achieve stability. Therefore, on each tack, once the trim position is found, the crew is kept standing still to assure a more reliable linearization for the control loop to exploit.

Theoretically, the two tacks are symmetric and we need the two linearization to have the same absolute value in each entry to achieve consistent Closed Loop behavior with the same set of weighting matrices thus consistent performance. On the other hand, being the set point $(\mathbf{x}, \mathbf{u})$ skew, the entries of the two vectors describing lateral related quantities need to change sign. Those entries are ϕ, ψ, p,r,v for the $\mathbf{x}$ and Δ_{flap},δ_r regarding the $\mathbf{u}$ and, although not specified in the control vector nor in the state, the X_{crew} position needs to change side. Note that the AoA_{sail} do not need to change sign due to the way the Lift is defined in the equation (2.19). however, since sail actuation switches reference on opposite tacks, it is necessary to have different entries on the $\mathbf{B}$ matrix. Performing a linearization around the two symmetrical set points does not assure that the two matrices have corresponding entries of the same absolute value due to the system share complexity and sensitivity to the trim and control vectors variation. Therefore, being the right tack developed after the Control Loop design and weighting process for the left one to assure a perfect symmetrical behavior, the $\mathbf{A}, \mathbf{B}$ matrices for the closed loop $\mathbf{A}_r$,$\mathbf{B}_r$ are defined as:

$$\mathbf{A}_r(i,j) = norm(\mathbf{A}_l(i,j)) * sign(\mathbf{A}_{linr}(i,j)) \tag{3.1}$$

$$\mathbf{B}_r(i,j) = norm(\mathbf{B}_l(i,j)) * sign(\mathbf{B}_{linr}(i,j)) \tag{3.2}$$

where the subscript "r" stands for the actual matrix used in the right tack, "l" stands for the left tack and "linr" stands for the matrix arising from the linearization on the right tack. With this method we imply that the sensitivity of the system is not enough to switch sign and we assure a symmetrical behavior of the control loop extending all the validity of the analysis made on the left tack to the right one.

Chapter 4

Optimal Control Problem

For the design of the autopilot we have used the LTI approach with Linear Quadratic optimal control method exploiting the linearization of the system around Trim condition. The LTI approach implies the MIMO architecture of the control loop.

$$\begin{cases} \dot{\mathbf{x}}(t) = \mathbf{A}\mathbf{x}(t) + \mathbf{B}\mathbf{u}(t) \\ \dot{\mathbf{y}}(t) = \mathbf{C}\mathbf{y}(t) \end{cases} \tag{4.1}$$

$\mathbf{x}(t) \in \mathbb{R}^n$ the state vector, $\mathbf{u}(t) \in \mathbb{R}^m$ input vector, $\mathbf{y}(t) \in \mathbb{R}^r$ output vector. The index of behaviour is defined on an infinite control horizon

$$\mathbf{J} = \int_0^\infty (\mathbf{y}^T\mathbf{Q}\mathbf{y} + \mathbf{u}^T\mathbf{R}\mathbf{u})\mathrm{d}x \tag{4.2}$$

with the condition

$$\mathbf{Q} = \mathbf{Q}^T > 0 \tag{4.3}$$
$$\mathbf{R} = \mathbf{R}^T > 0 \tag{4.4}$$
$$(\mathbf{A}, \mathbf{B}) stabilizable \tag{4.5}$$
$$(\mathbf{A}, \mathbf{C}) rivelable \tag{4.6}$$
$$\tag{4.7}$$

the stationary feedback

$$\mathbf{u}(t) = \mathbf{K}\mathbf{x}(t) \tag{4.8}$$

$$\mathbf{K} \triangleq \mathbf{R^{-1}}\mathbf{B}^T\mathbf{S} \tag{4.9}$$

with $\mathbf{S}$ solution of the Algebraic Riccati equation:

$$\mathbf{SA} + \mathbf{A}^T\mathbf{S} - \mathbf{SBR^{-1}}\mathbf{B}^T\mathbf{S} + \mathbf{C}^T\mathbf{QC} = 0 \tag{4.10}$$

$$\mathbf{S} \geq 0 \tag{4.11}$$

In our case $\mathbf{A}=\mathbf{A}(\mathbf{x}_\circ)$, $\mathbf{B}=\mathbf{B}(\mathbf{x}_\circ)$,evaluated at a fixed trim condition, are valid in a wide TWA range mainly due to the fact that the AWA remains bounded to small values ($<25°$). To assure proper tracking of a set point we introduce the concept of proportional+integrator approach in LQ that in classical control theory assures proper tracking and a good characteristic of robustness against low frequency disturbance and model parameters variation. We require that $\mathbf{y}$ tracks asymptotically with null error a set-point $\mathbf{y}_p$. We will assume that the output dimension is equal to the control vector $\mathbf{u}$, and suppose also that the integral of $\mathbf{y}$ is available $\mathbf{y}^f(t) = \int_0^t \mathbf{y}(t)\mathrm{d}t$ which implies $\dot{\mathbf{y}}^f_{(t)} = \mathbf{y}(t)$.

We can define now the "augmented state vector"

$$\mathbf{x}_a(t) = \begin{bmatrix} \mathbf{x}(t) \\ \mathbf{y}^f(t) \end{bmatrix} \tag{4.12}$$

The augmented system will be now:

$$\dot{\mathbf{x}}_a(t) = \begin{bmatrix} \dot{\mathbf{x}}(t) \\ \dot{\mathbf{y}}^f(t) \end{bmatrix} \mathbf{u} = \begin{bmatrix} \mathbf{A} & \mathbf{0}_{n\times m} \\ \mathbf{C} & \mathbf{0}_{m\times m} \end{bmatrix} \begin{bmatrix} \mathbf{x}(t) \\ \mathbf{y}^f(t) \end{bmatrix} + \begin{bmatrix} \mathbf{B} \\ \mathbf{0}_{m\times m} \end{bmatrix} = \mathbf{F}\mathbf{x}_a + \mathbf{G}\mathbf{u} \tag{4.13}$$

Extending the cost index function to our augmented system

$$\begin{aligned} \mathbf{J} &= \int_0^\infty (\begin{bmatrix} \mathbf{x}(t) & \mathbf{y}^f(t) \end{bmatrix} \begin{bmatrix} \mathbf{Q} & \mathbf{0}_{n\times m} \\ \mathbf{0}_{m\times n} & \mathbf{Q}^f \end{bmatrix} \begin{bmatrix} \mathbf{x}(t) \\ \mathbf{y}^f(t) \end{bmatrix} + \mathbf{u}^T\mathbf{R}\mathbf{u})\mathrm{d}x = \\ &= \int_0^\infty (\mathbf{x}_a^T\mathbf{Q}_a\mathbf{x}_a + \mathbf{u}^T\mathbf{R}\mathbf{u})\mathrm{d}x \end{aligned} \tag{4.14}$$

We can solve it similarly to the (7.8) with a feedback gain

$$\mathbf{u}(t) = \mathbf{K}_a\mathbf{x}_a(t) = \begin{bmatrix} \mathbf{K} & \mathbf{K}^f \end{bmatrix} \begin{bmatrix} \mathbf{x}(t) \\ \mathbf{y}^f(t) \end{bmatrix} = \mathbf{K}\mathbf{x}(t) + \mathbf{K}^f\mathbf{y}^f \tag{4.15}$$

where $\mathbf{K}_a$ is the optimal gain obtained through the solution of the Algebraic Riccati Equation of the augmented system.

$$\mathbf{S}\mathbf{F} + \mathbf{F}^T\mathbf{S} - \mathbf{S}\mathbf{G}\mathbf{R}^{-1}\mathbf{G}^T\mathbf{S} + \mathbf{Q}_a = 0 \tag{4.16}$$

$$\mathbf{S} \geq 0 \tag{4.17}$$

The entries of $\mathbf{x}$ chosen to be integrated in $\mathbf{y}^f$ are ϕ, TWA-HDG h,θ,v.

ϕ needs to be kept near the optimal one, since the boat is unstable on roll axis due to its windward heeling and as soon as the boat crosses ϕ=0 the $\dot{\theta}/\delta_r$ relation changes sign hampering the closed loop stability.

TWA-HDG (ψ) is mandatory to have a proper tracking and to keep the boat in a constant point of sail or in a defined direction.

The h has to be bounded between 0.10m at rest and 1.4m when the boat jumps out of the water. The boat can change altitude(h) freely within the bound with minor influence on the dynamics. The inclusion of h in $\mathbf{y}^f$ allows to reduce the proportional gain relative to the h error, thus relaxing the instantaneous tendency of restoring flight height allowing the proportional response to be focused on other parameters, knowing that a prolonged time away from set-point will increase the cost function, gently sliding the foiling height in the vicinity of the desired value (-0.7m) with time.

θ and v are chosen because their variation within the sailing envelope is very limited. Both values are in fact almost null in every trim condition, therefore, having both tracking 0 allows the vessel to maintain flight in all sailing points.

The standard method already described requires that the integrated vector $\mathbf{y}^f$ has the same dimension as the control vector $\mathbf{u}$ since to initialize the $\mathbf{u}$ it is necessary that $\mathbf{K}^f$ is a square matrix. In fact the trim-point is stable thanks to the couple $\mathbf{x_0}, \mathbf{u_0}$. Once we have chosen an $\mathbf{x_0}$ it is mandatory that the input vector is close enough to $\mathbf{u_0}$ to assure stability at $t = t_0$. We can start the simulation with the integrator offset

$$\mathbf{Int_0} = -(\mathbf{K}^f)^{-1}\mathbf{u_0} \tag{4.18}$$

such that:

$$-\mathbf{K}^f\mathbf{Int_0} = (-\mathbf{K}^f)(-(\mathbf{K}^f)^{-1}\mathbf{u_0}) = \mathbf{I}_m\mathbf{u_0} = \mathbf{u_0} \tag{4.19}$$

The necessary variables to achieve a stable flight are ϕ near the optimal one, h within bounds and a defined direction of sail. The other variables have been chosen just to fulfill LQ requirements to assure a square $\mathbf{K}^f$ and θ should in fact vary with the boat speed.

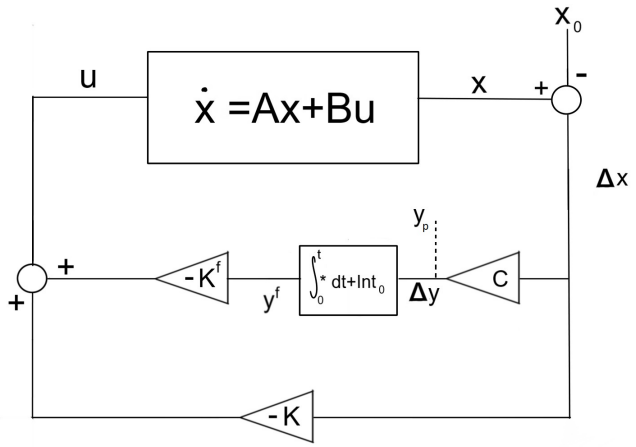

Figure 4.1: Proportional Integrator OCP

The inclusion of $\theta, \mathbf{v}$ in the integrated variables introduces unnecessary error in the integrator, depleting the architecture's power to keep the relevant variables on spot and degrading the closed loop performance, since an irrelevant error on θ will hamper ϕ,TWA,h tracking increasing instability and splash down probability. To reduce this effect as much as possible, it is possible to decrease the unnecessary variable weight in the $\mathbf{Q}_a$ matrix. On the other hand, bad conditioning of the Open Loop $\mathbf{A}$ matrix (conditioning number$= 4 * 10^4$) implies that the various weight in $\mathbf{Q}, \mathbf{R}$ cannot be freely chosen to assure a solution to the Riccati equation. The $\mathbf{K}^f$ generated in this way is bad conditioned as well, therefore, its inverse behaves badly determining the initial status of the integrator, resulting in a prolonged transient with oscillation of the state vector around $\mathbf{x}_0$ even when the initial condition of the simulation is exactly the trim one. The simulated time hardly exceeds 50s due to huge CPU demands from the model, therefore, other paths have to be explored. A different set of integrated control variable has been tried (ϕ,TWA,h,w_b,v_b) and found to be an improvement that shows more numerical stability and allows us a better control at different boat speeds. As a rough approximation, considering

fixed the integrated variable (θ or w_b)

$$L = \frac{1}{2}\rho_{water} S C_{l_\alpha} \theta u_b^2 \tag{4.20}$$

$$L = \frac{1}{2}\rho_{water} S C_{l_\alpha} w_b u_b \tag{4.21}$$

we can see how by fixing w_b we have less variation of Lift with respect to velocity. Therefore, we can extend the envelope where the same x_{ref},u_{ref} set-point can be used in different TWA,TWS. Still, the complexity of a classical control loop, the bad conditioning of the linearized matrices and the heavy load on the computational requirements (especially for the initial educated "guessing" phase) inspired an empirical approach outside of the classical theory studied.

4.1 Different Approach

Given the already discussed classical approach limitations in weighting choice, computational power shortage and sub optimal performance, and that any improvement is time consuming due to slow simulation, we explored other solutions to try to enhance the closed loop behavior and have results in a reasonable amount of time, especially for the initial guessing game of tuning. To improve performance and reduce computational requirements we focus on integrating just the 3 variables worth of: ϕ,ψ,h; With this architecture we are no longer able to determine an integrator offset that produces the desired input from the beginning, since $\mathbf{K}^f_{m\times n}$ has no inverse. Starting the simulation with an input $\mathbf{u} \neq \mathbf{u_0}$ will end up in catastrophic results, so the $\mathbf{u_0}$ is added to the input practically shifting the null input around the $\mathbf{u_0}$ vector.

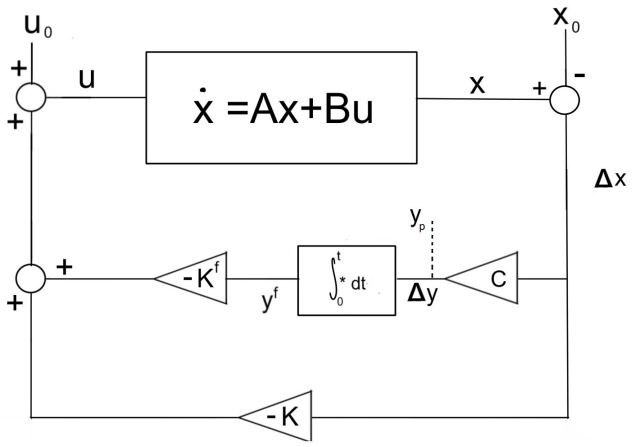

Figure 4.2: Modified Proportional Integrator OCP

Provided that the boat at $t = t_0$ is stable with the trim input for some seconds, we can assume that the control loop will

take over on the simulation correcting the input in response to any state deviation from the trim state $\mathbf{x_0}$ while the simulation progresses. With this architecture we are allowed to increase the range of weighting choice thanks to a more stable numerical computation of the solution of the Algebraic Riccati equation. Therefore, we are able to tweak the closed loop behavior to achieve the desired response. Once we found a viable set of weight, we will try to extend those choices to the classical schemes with minor adjustments hoping for the viability of the Algebric Riccati equation solution and achieve good performance with minor tweaks on few variable in not many simulation runs.

The skewness of the problem implies that the $\mathbf{y}_p$ can only be used, reliably, when *psi* refers to TWA and the variation of TWA remains within the same tack limit. Although possible to tack with $\mathbf{y}_p$, the presence of a non zero $\mathbf{x}_0$ coupled with the non linearity of the problem and the cross coupling of forces and moments along different directions do not guarantees a symmetrical behavior during maneuvers due to the proportional component of the closed loop architecture. The behavioral uncertainties,during maneuvers, are magnified by the necessary scheduler on the control loop. To assure a symmetrical and reliable behavior during tack and jibes it is preferable to use directly the $\mathbf{x}_0$ to change course. The slight overshoot that arise by using $\mathbf{x}_0$ to perform the maneuver is in fact beneficial allowing the boat to accelerate after the maneuver in a broader TWA.

4.2 Modes of control

To unlock full potential of a control loop for a sailing dinghy, given the physical limitation of such kind of vehicle, different modes must be designed with specific sets of variables to be controlled. In this work we developed 3 different working modes:HDG lock,TWA lock,VMG; Each of them can be run standard or Forced Fast. The standard mode uses the trim state vector as reference. Therefore, after changing conditions i.e. wind intensity increases, the boat should accelerate freely, while, with a constant reference, the acceleration will be hampered by sub optimal trim point even with low weighting of the boat speed. To overcome this limitation, the Forced fast mode has been created with a constant error on the speed coupled with an increase of weighting of θ error since such variable experiences an undesired variation. In this mode, although the total error will increase (with negligible reduction in stability), we assure by design that the control system will force the speed to its upper limit bounded only by the physics of the problem in closed-haul condition ($\mathbf{x}, \mathbf{u}$,wind). The gain in velocity is marginal because the trim speed is near the maximum allowed. However, in other conditions, like a sailing point shifted even by few degrees towards beam reach, we can see an increase in boat speed between the two modes of few knots(i.e. 2.3 kn **@**TWA=68°) due to the fact that the speed entry in the state vector differs significantly to the max speed physically achievable.
The HDG and TWA lock modes are theoretically the same, since the physics of the problem do not change strictly with the heading but are related to the TWA. The difference on the state vector is the definition of the 3^{rd} component (ψ). In the HDG mode it is defined as the angle between the x_b and the north direction, where the TWA is defined as the angle between x_b and the true wind direction. The first mode is very useful to navigate, since its reference is directly connected on to the **NED** frame of reference that can be easy translated to navigation coordinate system

(λ,φ), while the latter can be exploited in shifting conditions to assure that the boat keeps a stable point of sail. With north wind the two definitions are in fact the same. In shifting wind conditions where the destination is outside the sailing envelope, with TWA locked on close haul or broad reach, the closed loop is able to exploit a "lift" or an 'header' to increase the velocity in the target direction. To achieve TWA lock it is mandatory to know the wind direction that in practical condition is not granted. In this model, TWA is evaluated performing the rotation in ϕ and θ of the apparent wind

$$TW_v = R_\theta R_\phi (AW_b - V_b) \tag{4.22}$$

the vertical reference frame allows us to bound the wind vector in the horizontal plane where the computation of the angle is straight forward. The evaluation of TWA is numerically unstable at the beginning of the simulation. In order to avoid this issue, a linear,time proportional scheduler shifts from HDG to TWA reference in the first seconds of simulation .

The VMG mode introduces in the state vector another variable which is $1/v_{e_n}$, which assumes that the target is north-wise of the boat. Although not implemented, the same concept can be applied on different directions. The closed loop in VMG is proportional. Using the inverse of VMG instead of VMG by itself allows us to maximize the VMG both in up wind and down-wind direction with the same algorithm by directly minimizing the $1/VMG$. Using this mode implies to discard the HDG-TWA error integrator for obvious reasons. The VMG mode shows a less stable behavior and high sensitivity to parameters variation but allows us to find the best TWA (fixed north wind) in order to maximize the upwind/downwind velocity component. The lower stability of such mode of control means that it has to be used wisely. The best use is to switch from the HDG mode to the VMG mode while in close reach for a short period, and save the new set-point as reference or, in preliminary phases, to collect useful set points

with a reduced (more stable) model. Once the new set-point $\mathbf{x}, \mathbf{u}$ is found we can switch back to the HDG mode on the new set-point. This procedure can increase the performance of the boat by finding on the go the sweet spots for sailing without necessarily going through all the possible TWAs at any given TWS to store the data of the polar chart and use those charts as reference to evaluate the appropriate point of sail. Extra care needs to be addressed while exploiting this feature in low wind, since the boat tends to sail too close to the wind with an exaggerated θ resulting in a sailing condition where the sail thrust is just shy of the equilibrium one, consequently, the boat will start loosing speed. In this case the VMG mode tries to gain VMG by heading up and setting itself in a less powerful condition entering a vicious loop that ends up with a loss of flight: once the boat is too close to the wind, heading up or bearing away have transient results,VMG wise, that are opposite to the long term result. The linearization procedure tends to discard the long term evolution focusing on instantaneous effect. To overcome this issue it is mandatory to start the VMG away from the optimal TWA with low weighting of the VMG to have a quasi static rotation towards the best angle. Still, the best use of this mode was in the preliminary phase of this thesis, where a bunch of different trim condition were found with a reduced model without the inertial torques(2.31 equation) where the vehicle experienced a more stable behavior. Once the complete model is simulated the VMG mode is barely stable and its hampered effectiveness is not guaranteed in all conditions. Thus, a more classical approach with wind intensity interpolated polar charts produced experimentally or by simulation offers more reliability and sturdiness and is, therefore, suggested. Since the eq:2.31 affects stability but not performance, a finer analysis can be performed in the vicinity of the best performing TWA to properly characterize the polar charts near their best.

Another mode has been explored with scarce results, AWA locked. This mode is supposed to have outstanding performance,

having the sail physics directly correlated with such angle, and is very common oh high end sailboat autopilots for racing yachts. The AWA variation are highly dependent on different 3D vectors sum, therefore, multiple gain matrices should be scheduled with TWA & boat speed to take care of the different behavior of AWA in various conditions. A first attempt in closed haul has been tried out, but as a matter of fact the intrinsic noisiness of such signal, practically related to TWS ϕ p,q,r TWA, $\mathbf{V}_b$ coupled with the definition of the sail actuation, AoA instead of the classical sheet and pulley, means that a stable closed loop can not be found. An interesting consideration can be made on the sail actuation. The direct AoA control eliminates the need of mathematical model for the sheet's slack but compromises the AWA stability. In a classic sailboat, an increase in speed, thus a reduction of AWA, will decrease the AoA of the sail, since its position is fixed to the boat reference. Such reduction will reduce heeling and boat thrust, both inducing an increment in AWA restoring the initial condition and vice versa. The direct control of the AoA means that a change in AWA will physically rotate the sail that now has as reference the Apparent Wind Angle, and the rotation of the resultant alone (present in the classical control scheme but negligible with respect to the AoA effect) is not enough to have proper stability. The noisiness increases the difficulty to produce a well behaving feedback loop on such variable. On top of that, the natural heeling stability on this foiling boat is negative and the AWA is bounded, in trim conditions, between 14° & 22° while on a classic sailboat it can easily go up to 140°. In practice the reduced stability and the highly reduction of signal/noise value for an AWA Control Loop dissuade further efforts to develop working gain matrices for such parameter.

4.3 Weighting choice

The Weighting choice for the standard PI LQ OCP, as already mentioned, was mainly driven by MATLAB capability of solving the associated Algebraic Rccati Equation, and proceeded as an exhausting try and error session where the best achievement results in warnings for bad conditioned matrices. With little to no room for spares, the behavior of the closed loop was in some way limited by its numerical constraints. On top of that, the forced choice of the fifth integrated parameter (θ)[1] results in a sub optimal behavior. Due to heave limitation,the height of the boat from the water surface while foiling is bounded to be between [0.15m to 1.4m) [2], θ in any trim condition can be traced to α one of the angles which define the DCM_{bw}. As any pilot could tell, with the variation of speed, an airplane has to adjust $\alpha \rightarrow \theta$ accordingly to maintain steady level flight. Where a foiling boat and an airplane differ is in the thrust generation. In our case we cannot set a fixed thrust, and the propulsion from the sails depends on many factors such as boat speed, relative angle to the wind, wind intensity,heel angle... since the purpose of this project is to find a closed loop that stabilizes the foiling of the boat in the widest range of TWA and TWS, rather than a simple gust response in a singular trim condition. We can figure out where the shortcomings of this method lay. Different considerations can be made on the w_b arrangement. In this case, the weighting choices, still limited by the ARE solution existence, have a broader range and showed good performance at different boat speeds.

Once we have found the right combination of weights on the $\phi\psi$h loop we tried to directly transfer them onto the two classical PI LQ loops. The one integrating θ did not accept the weighting

[1] the θ parameter is shown as fourth on the weight matrix choice to respect its appearance in the $\mathbf{x}$ vector but has been chosen at last

[2] in heeled condition the maximum height is even reduced since it is necessary to avoid as much as possible the surface piercing of the main foil tip that introduces, due to extrados suction, air bubbles around the wing causing ventilation with effects similar to a stall

State Variable	ϕ ψ h θ v_b	ϕ ψ h	ϕ VMG h	ϕ ψ h w_b v_b
ϕ	$\frac{180}{\pi}$ 0.5	$\frac{180}{\pi}$ 0.5	$\frac{180}{\pi}$ 2	$\frac{180}{\pi}$ 0.5
θ	$\frac{180}{\pi}$ 0.1	$\frac{180}{\pi}$ 30	$\frac{180}{\pi}$ 2	$\frac{180}{\pi}$ 30
ψ	$\frac{180}{\pi}$ 9	$\frac{180}{\pi}$ 110	$\frac{180}{\pi}$ 20	$\frac{180}{\pi}$ 110
p	$\frac{180}{\pi}$ 10	$\frac{180}{\pi}$ 70	$\frac{180}{\pi}$ 0.2	$\frac{180}{\pi}$ 70
q	$\frac{180}{\pi}$ 1	$\frac{180}{\pi}$ 5	$\frac{180}{\pi}$ 2	$\frac{180}{\pi}$ 5
r	$\frac{180}{\pi}$ 1	$\frac{180}{\pi}$ 11	$\frac{180}{\pi}$ 0.02	$\frac{180}{\pi}$ 11
u_b	0.001	100	0.001	100
v_b	0.1	0.1	8	0.1
w_b	0.01	0.1	0.01	0.1
h	1	1	1	1
ϕ^f	$\frac{180}{\pi}$ 4	$\frac{180}{\pi}$ 4	$\frac{180}{\pi}$ 2	$\frac{180}{\pi}$ 4
ψ^f	$\frac{180}{\pi}$ 6	$\frac{180}{\pi}$ 6	-	$\frac{180}{\pi}$ 6
h^f	0.05	0.05	0.001	0.7
v_b^f	0.03	-	-	0.03
θ^f	$\frac{180}{\pi}$ 0.01	-	-	-
w_b^f	-	-	-	0.01
VMG	-	-	100	-
AoA_{sail}	5	5	1	5
mean_{flap}	1	1	0.08	1
Δ_{flap}	1	1	0.08	1
δ_t	0.5	0.5	0.05	0.5
δ_r	300	300	15	100

Table 4.1: Different weights

choice (ARE solution ∄) and, after few adjustments, we managed to compute the optimal closed loop gain but we ended up with degraded performances and we discarded that architecture. The more promising $\phi\psi$h$w_b v_b$ accepted the weighting choice and, with few runs to proper weighting v_b, w_b, we ended up with a good performing optimal gain without the time consuming process of developing them from zero on a more computational demanding architecture. As we can see, we have changed also the entry relative to h^f. This necessity arose during tack simulation (the lower weight was enough in straight line) since the small weight ,sufficient in the reduced integral control loop to keep the flight height constant, paled when compared to the new integrated variables. Moreover, w_b somehow interferes with the h value, especially when the tacking swung the boat from side to side. A side effect of the increased weighting appears in high wind, where the relevant error in h^f interferes with the two main parameters needed for a stable flight $\phi\psi$, The incresed integral error develops an intermittent non-transient oscillation that disappears after many seconds. We accepted a trade off where, at TWS=12m/s, after a maneuver we had those oscillations (in a calm sea state) for 100s with period$\sim$1.7s and $\Delta\phi \pm 0.25°$ $\Delta TWA \pm 0.5°$. The architectures were tailored in "forced fast" mode, in such a way that the weight relative to u_b and its constant -1 error were carefully chosen to increase the boat speed when possible without interfering too much with the other variables.

We can look at the $\mathbf{x}$ entries in such a way that a simple Proportional feedback loop can in fact act similarly to a Proportional Derivative feedback loop. Even if not strictly true due to rotation 2.48, we can assume that increasing the p weight will reduce the ϕ rate of change while the q will act similarly on θ and r on the ψ. Therefore, an overshoot on Euler angles can be dampened with increased weight in corresponding rotational rate. As we can see from the Tab: 4.1, we had substantial overshooting in ϕ and ψ while the θ angle needed a fast proportional response but with

an already dampened behavior. An important consideration can be made on $\mathbf{R}$ entries. The exaggerated weight of the δ_r stands out, this choice was dictated by design trade offs and personal experience. The rudder by itself is hydro-dynamically too big for such a small dinghy, its dimensions were imposed by structural constrains, the length has to be the same as the main foils struts to have the same draft during foiling. The chord, related to the thickness by the foil shape, was needed to withstand the side loads and the compression arising from the t-wing at its tip. The absence of a hull into the water, coupled with rudder long leverage, increase its effectiveness having little to no rotation resistance provided by the hull nor by the two struts. Similar dinghies have analogue problems with oversensitive rudders, therefore, the high actuation cost reduces the rudder deflection as much as possible, keeping the boat stable in both ψ and ϕ[3].

The VMG mode is based on a more stable platform and its only purpose is to find optimal trim condition through a reduced model. It presented less complexity during the weighting process and it produced various trim points with best VMG in different wind conditions, but its performance as control loop on the full model has scarce to no meaning. From now on, the control loop with $y^f = \phi, \psi, h, w_b, v_b$ will be referred to as "Complete integral", while $y^f = \phi, \psi, h$ will be the "reduced" one.

[3]the center of pressure of the rudder is far away below the boat since the airborne section has no effect, -δ_r induces a positive yaw and has a side effect on roll inducing a positive rotation

Chapter 5

Gain scheduling for Tack/Jibe maneuver

The gain scheduling was attempted with one sentence in mind :"the model does not react well to discontinuities" A tacking maneuver is defined as the change of tack crossing the up wind direction. From one tack to the other a dinghy needs to switch sign of ϕ and move the crew from one side to the other, and needs to do that in a continuous way $\dot{\mathbf{x}}(t), \mathbf{u}(t) \in C^0$. The eccentricity of the CG with respect to the body FoR origin means that any discontinuity will induce an undesired torque, resulting in a bad maneuver. The simulation struggles numerically as well, therefore, extra care on continuity has to be taken. The main source of discontinuity to be addressed is the sail lift definition 2.19, where the sign function presents two huge discontinuities near AWA =0. Since the lift at low AWA generates mainly a side force, and the AoA remains nearly constant during the whole maneuver due to the input definition, once we approach AWA $\sim$ 0 the sail lift changes abruptly side inducing roll motion and sway in a manner that makes the AWA change sign again and again

Making the boat shake back and forth interrupting the simu-

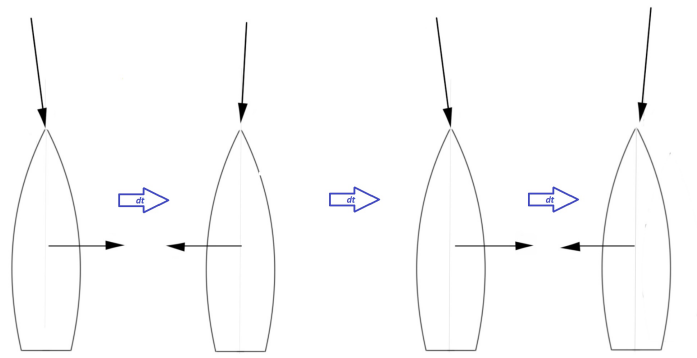

Figure 5.1: Tack Sail Force Oscillation

lation. To avoid this we substitute the sign function in 2.19 with

$$sign(AWA) \rightarrow \frac{2}{\pi} tan^{-1}(100AWA) \tag{5.1}$$

The 100 factor is in place just to assure that up until the taking moment the sail force is as similar as possible to the one described by the original function. In fact, the sail force is 97% of the original description with AWA = 28°[1].

[1] $\frac{2}{\pi} tan^{-1}(100AWA)$ function is defined inside the $C_{l_{sail}}$ to avoid the "ghost" of the induced portion in the drag equation.

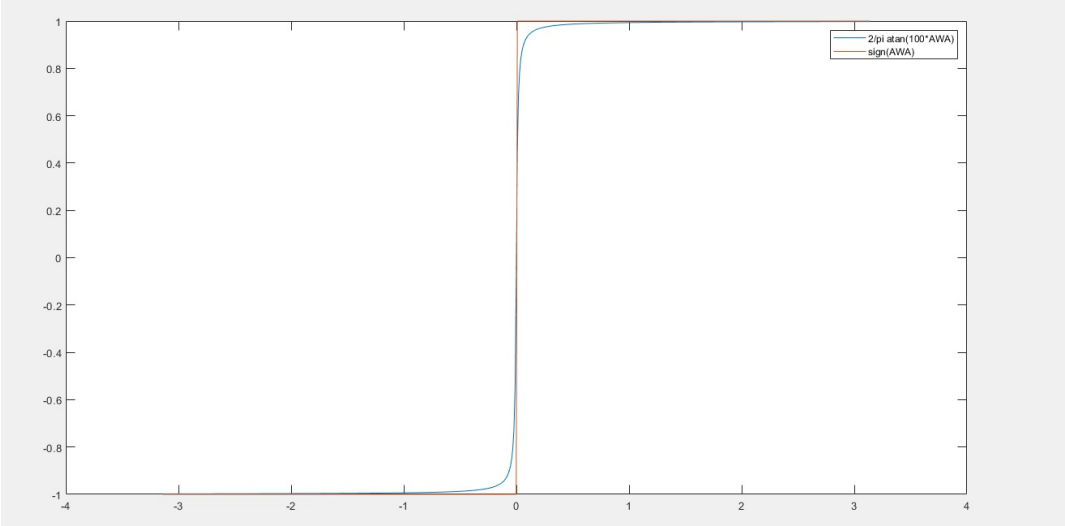

Figure 5.2: Sign Vs $\tan^{-1}$

With the smoothing of the sail lift function with respect to AWA, the simulation does not experience abrupt interruption near the tacking dead center having $\lim_{AWA \to 0^{\pm}} = 0$. The high rate of change still increases the computational power needed to complete the simulation.

As we have seen in 2.21 2.22 2.23, ϕ optimal is strictly related to the ratio between the lateral force that the crew can overcome by equating heeling and righting moment and the total weight of the boat. Therefore, since those variables are related to the geometry of the boat, we can assume a constant angle across all the points of sail. On the other hand, during a maneuver we know that the boat has to roll switching sign of ϕ, at the same time the crew has to change side. We know that the sailboat cannot foil indefinitely in irons nor in dead running, therefore, once the boat sails closer to the wind than what usually is referred to as "high mode" (in upwind) which is, loosely speaking, the lowest TWA, where the sailing can continue indefinitely, there is no point in keeping squeezing performance out of the vessel since we will end up loosing flight no matter what. A similar reasoning can be applied on down-wind situation approaching a

jibe, when TWA lays inside the dead zone . By experience, on the simulated model the dead zone spreads around $\pm 45^\circ$ from the wind direction. With this in mind we can allow the crew to switch sides and consequently ϕ in this range. We can set a simultaneous "smooth"[2]transition between the optimal feedback gain evaluated for one tack to the other. As we will see later, the actual range where the gain transition occurs does not cover the full $\pm$ 45° sector deemed to large. When the maneuver occurs, the reference state vector needs to change ϕ sign since this is the only variable of $\mathbf{x}$ that sensibly differs from 0 (p,r=0; v$\simeq$0. While the other variables stay constant) to achieve a variation on ϕ and Y_c both entries on the reference state vector($\mathbf{x}_{ref}$) are modeled as f(TWA) evaluated by the model

$$Y_c = -3sin(TWA) \tag{5.2}$$

Given that theY_c position is bounded geometrically to $\pm$2.10m by the boat dimensions, we can assume that the crew saturates its value at TWA$\simeq \pm 45^\circ$, similarly, on the ϕ angle we know that on trim condition it should go to $0.3_{[rad]} \simeq 17.18^\circ$. To assure a proportionality between Yc and ϕ we define the reference as

$$\phi_{ref} = -\frac{3}{2.1/0.3} sin(TWA) \tag{5.3}$$

In the scheduler designed for this application, when the boat crosses the TWA=0 the feedback loop gains are an average of the two gains computed for straight sailing. We assume that the linearization matrix across the dead zone is a linear combination of the two sides matrices, even if it is not guaranteed, since through the feedback loop robustness and low sensibility of parameters variation we can complete the maneuver.

[2]mathematically speaking the right terminology should be "continuously", since the derivative of the switching function has discontinuities when the switch engages or disengages, but in the text it could imply a back and forth switching which is a wrong assumption

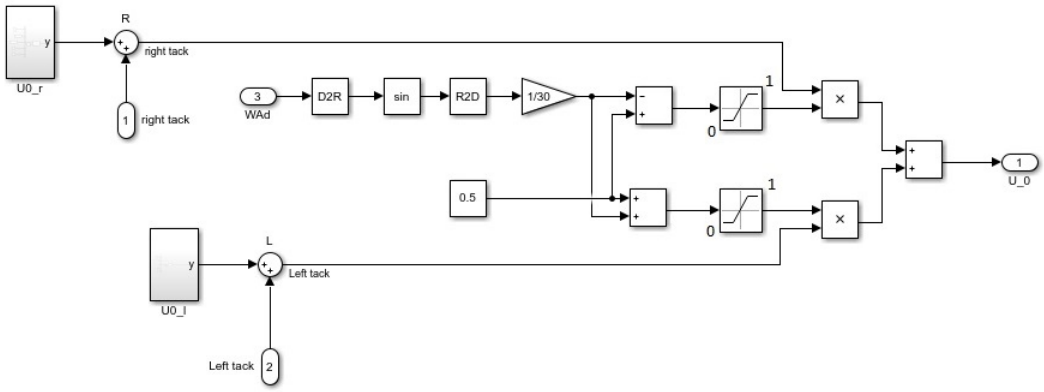

Figure 5.3: Scheduler

As we can see in 5.3, we have the two $\mathbf{u}_0$ relative to the trim condition on opposite tacks, the two inputs(1,2) that are the control vectors arising from the feedback loop and the variable WAd, which is TWA expressed in degrees, that acts as switching variable. The gain scheduling occurs between $\pm 15°$ and as we can see in the figure the switching function is

$$F_{switch}(TWA) = 0.5 \pm \frac{6}{\pi} sin(TWA) \tag{5.4}$$

with saturation block allowing the interval [0,1]. Since:

$$sin(TWA_{[rad]}) \simeq TWA_{[rad]} \tag{5.5}$$

$$\frac{180}{\pi} sin(TWA_{[rad]}) = TWA_{[°]} \tag{5.6}$$

The introduction of sin function allows us to use the same scheduler developed for the tack during the jibe, since sin(TWA) around π behaves similarly to 0 and the crew movement and ϕ still needs to switch side an ϕ sign. The main difference between

a tack and a jibe is the definition of ψ. To induce a jibe while in left tack we need to increase the TWA to a value greater than $180°$, the closed loop tracks the reference value, but as soon as the boat crosses the downwind direction the TWA evaluated in the model changes sign $180°^{+} \rightarrow -180°^{-}$ due to the "atan2" built in MATLAB function definition. Therefore, the error changes accordingly $\delta_{\psi} \rightarrow 2\pi + \delta_{\psi}$. To overcome this issue at the crossing the reference ψ is corrected to $\psi - 2\pi$ through an if block. It has to be noted that this last feature works only for testing and it works for a jibe from the left tack to the right tack, or for a jibe in both directions with the addition of a symmetrical if code line, but, in the latter case, not for tacking. A more complex and robust solution for a reliable practical implementation has yet to be found. The simulation shows that, aside this kind of numerical hiccups, model and scheduler behave well in both tack and jibe starting from a left tack. The symmetry of the model guarantees that the same behavior has to be expected starting from the right one.

We remark that during tacks the architectures were always in "forced fast" mode, where the boat speed is always gently pushed faster.

Chapter 6

Simulation

The simulation of the model suffers numerical instability. Especially away from trim condition, the complex interaction among all axes aggravates this issue. Different time advancement schemes had to be used in different phases of the project. During the preliminary Trimming phase the simulation performed better in a fixed time-step (10^{-4}s ode3), while, once the trim was found and the simulation relied on closed loop optimal gain feedback, an ode45 variable size step method gave the best results in terms of run time (machine) in various conditions: straight line at different points of sail , head-ups, bear-aways, tacks and jibes both in calm or "heavy" sea state, stable or shifting wind both in speed and direction. In some cases the variable step (ode45) still suffers from numerical instability, especially with the full integrated feedback. Switching back to a fixed step integration (ode3 with a fixed step of 10^{-2}) will solve the problem.

6.1 Wave response/rejection

Usually mechanically driven SISO feedback loops on heave stability, already common in wide spread small foiling dinghy, as can be seen in Fig:1.3, rely on a stick called "wand" that acts like a feeler reading the distance between its pivot point and the sea surface and directly actuating the only flap present in the main foil through a set of rods and rockers. The mechanical SISO relies on high proportional gain to limit the vertical offset from nominal height in different sailing conditions. The mechanical layout in small boats have the constraint of extreme light weight construction, therefore, only proportional response can be achieved. In any wave condition the response of such system is felt too harshly by the sailors who tried it. Any non surface-piercing foiling boat is able, in theory, to cut through waves smaller than its strut draft with minor effort. The stiff response can be traced back to the mechanical layout and the difference in height between the sea surface and the sea level. In fact in larger foiling boats (i.e. AC55, AC75) where a crew member is deputed only to the flaps actuation , thus the flight height, experience a smoother sailing in rough seas. In our case we neglected the physical modeling of sensors, therefore, we can rely on the flight altitude arising from the **NED** inertial frame. Our description, although theoretical and not necessarily of easy implementation in the real world, provides a great increase of stability in the sailing envelope. The Fig:6.1 shows the difference between a pure inertial h in the state vector on top and an h+$h_w(\omega t)$ on the bottom. The latter represents the case where h is read by a surface skimming probe.

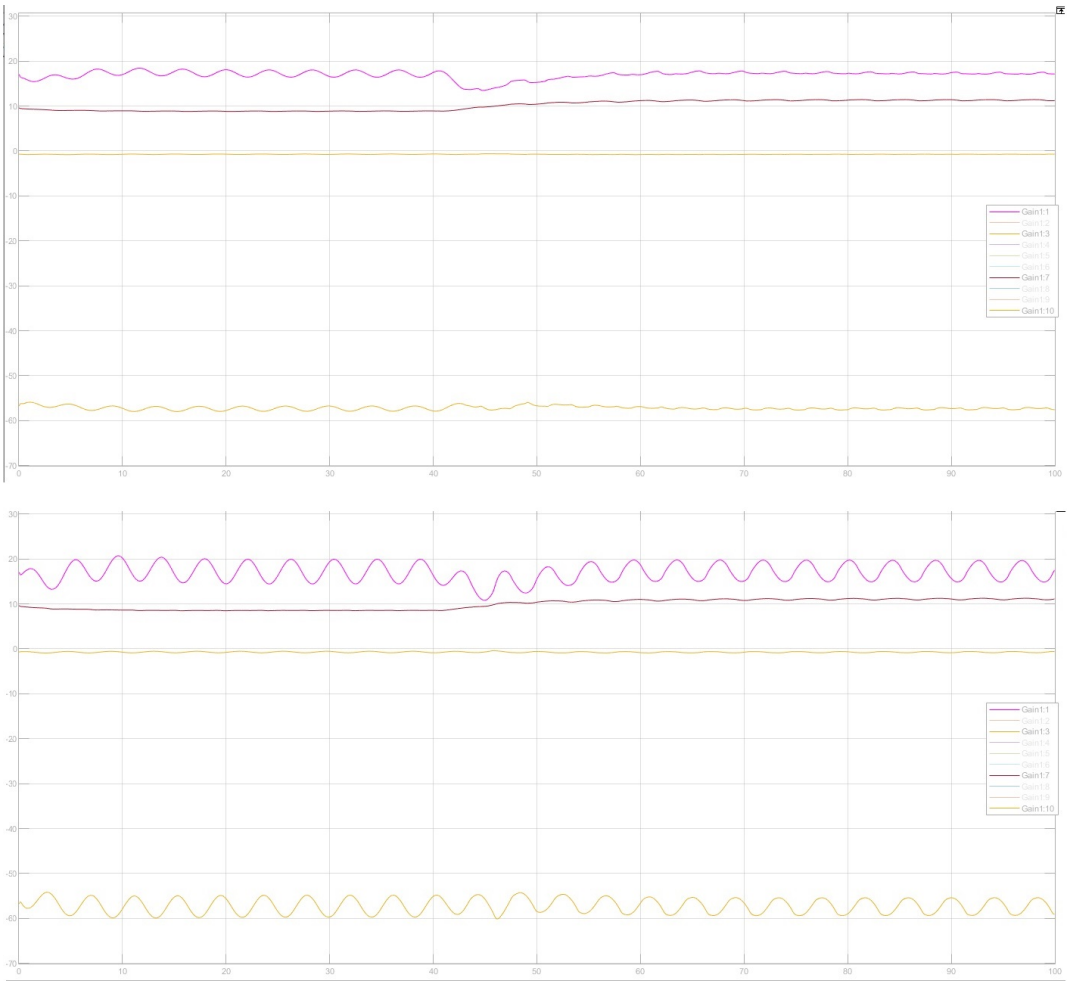

Figure 6.1: Wave response

In this specific simulation there is a gust (at t=40s) that doubles the TWS (4 $\rightarrow$ 8m/s). While the wave height is constant at 0.6m wave lenght 40m the highlighted variables are from top to bottom ϕ, V_{b_x}, h, ψ. In most of the circumstances the purely inertial h performs better, since all the correction in inputs are related to inertial motion and actual parameters variation, while in the second case the closed loop reacts to a constant change in the h value due to free surface motion. The only case where a wand system can outperform an inertial frame reference is in an elongated swell situation, when the wave height is comparable or grater than the strut dimension (1.4m in our case). In this peculiar case a hybrid system of an inertial reference, coupled with a low frequency direct reading of the foiling height, could improve the feedback loop response allowing the system to track the swell's wave profile while rejecting the small chops as disturbs.

6.2 Tack/Jibe simulation

Tack and jibe are complex maneuvers which involve a huge mass displacement and a sensible change in parameters of the state vector. During maneuvers the boat has to sail trough a range of TWA, where prolonged sailing is not possible and the sails have to switch sides. In regattas the crew which is able to perform faster maneuvers usually ends up in a better position. Indeed, during training large part of exercises involve maneuvering. In foiling boats tacks and jibes have the increased complexity of maintaining a stable flight with no thrust on an unstable platform with a plethora of cross coupled actions, i.e. the active part of the rudder is far below the center of mass and the lateral force experienced during the turn means that the side-slip angle β increases the lift produced by the vertical struts causing an inverse roll motion, while the hull has to be kept clear of the water to avoid additional drag. In sailboats the maneuvers are usually timed carefully with the sea state to reduce the speed loss as much as possible. Our scheduler approaches the tack in a simplistic way (time based) and has been tested in a somewhat reduced range of situations, but is still enough to comprehend the features and limitations of the platform. When the boat sails in irons or running downwind, the trim linearization is still valid for the underwater description but the relation thrust/ψ is completely misrepresented. Therefore, outside the TWA envelope the linearization keeps the boat stable for a short transient, while the vehicle loses speed due to a lack of propulsion and inevitably exits foiling condition.

In the Fig:6.2 we can see two consecutive tacks in changing wind condition. We perform the first (left $\rightarrow$ right) in TWS 4m/s and the second (right $\rightarrow$ left) in TWS 8m/s, allowing us to evaluate at a single glance two wind conditions and the response to a gust in a single simulation. As we can see, the two different closed loop configurations perform similarly with the already cited intermittent oscillation on the complete integral scheme (graph on the bottom). In rough sea state the two closed loops behave in a

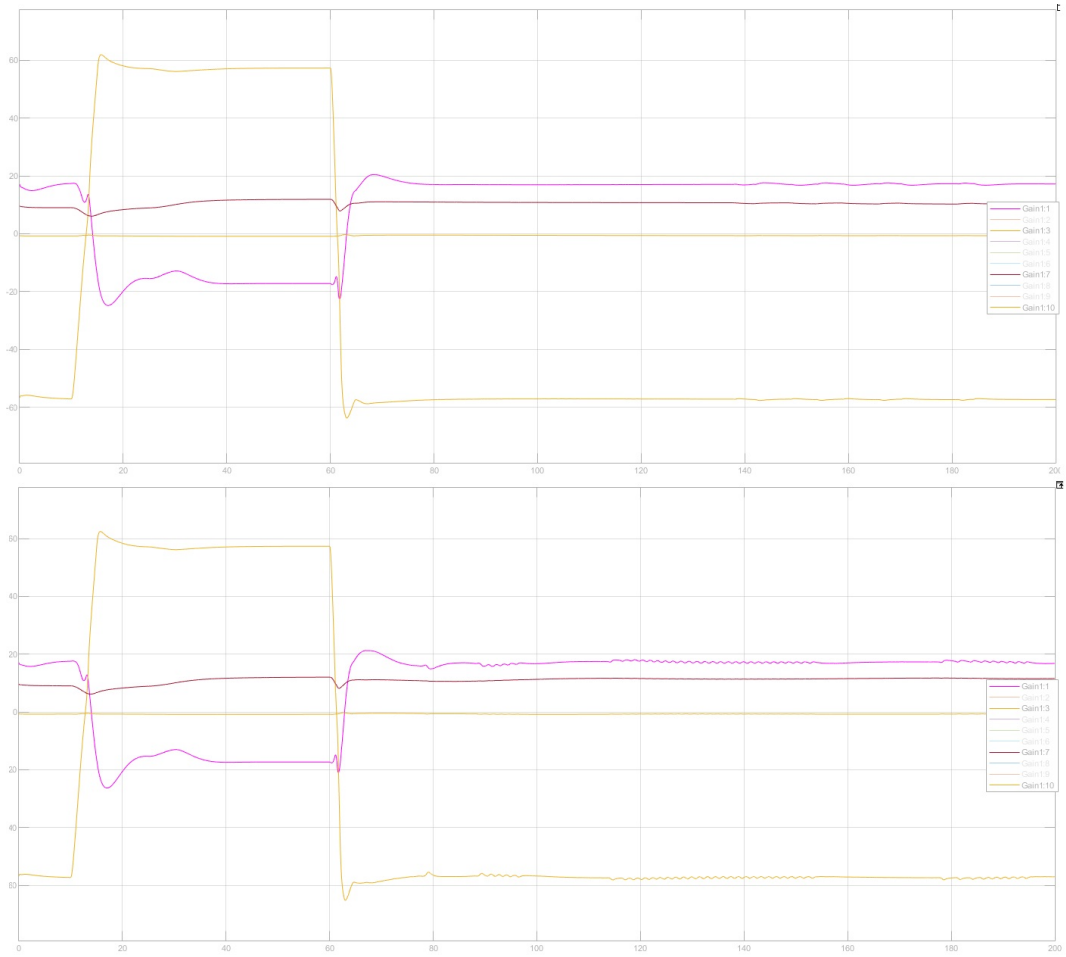

Figure 6.2: Tack maneuver in calm sea

similar manner with a slight improvement on the complete one.

We can see the difference between the two different closed loops reduces in rough sea condition.

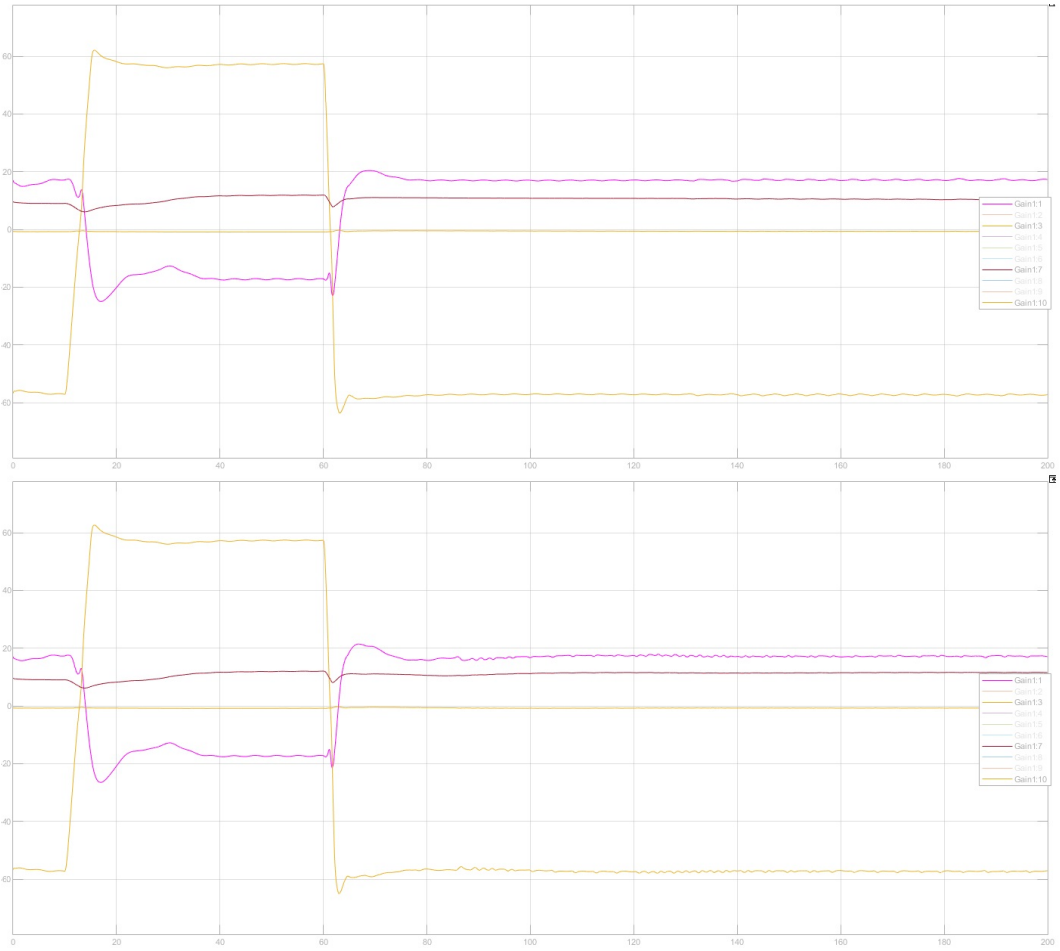

Figure 6.3: Tack maneuver in 0.2m waves

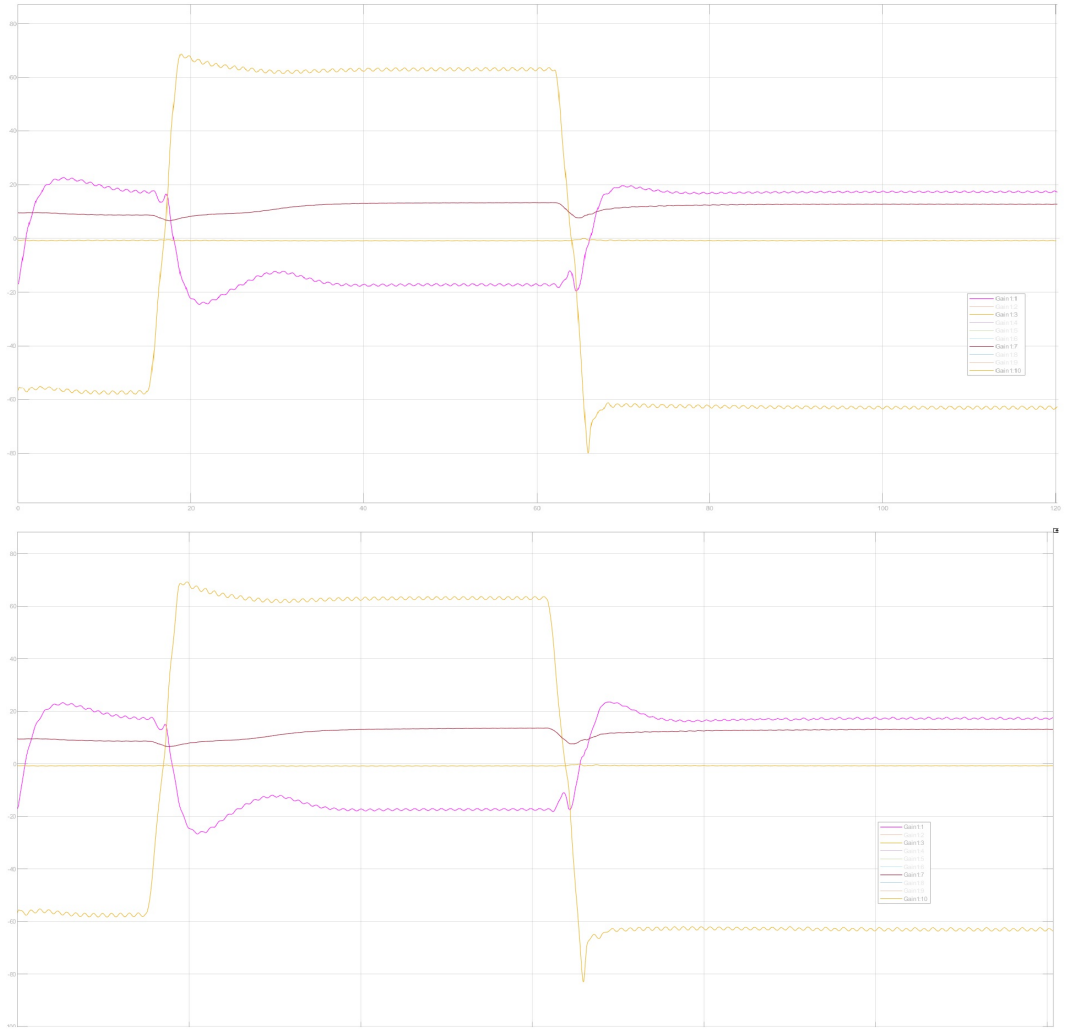

Figure 6.4: Tack maneuver in 0.6m waves

The wind condition at which the maneuver occurs changes drastically the behavior, in fact, especially in high winds, the tack presents increasing difficulties. Once the boat is in the dead zone it experiences a huge amount of drag[1], since the aero-drag is proportional to $(V_{b_x} + TWS)^2$ in high wind, the boat smashes into a wall of air during its most critical phase. To avoid that, a faster maneuver can be performed with the down-side of an intense cross coupled roll. With increasing TWS, the boat is cornered in a lose-lose situation where a tack is performed too fast regarding trajectory and lateral Gs, and too slow when considering the aero-drag related loss of speed.

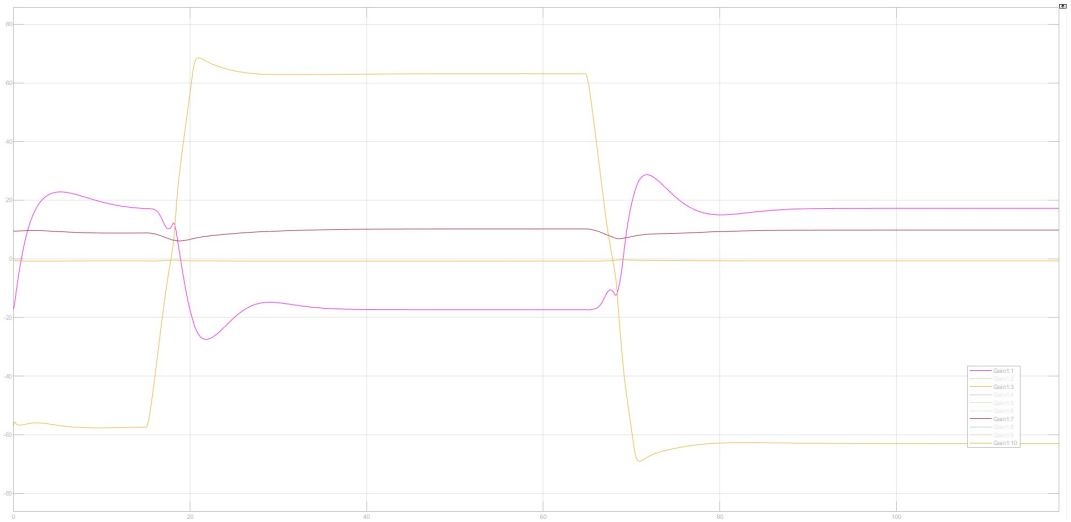

Figure 6.5: Two well performed opposite tacks in the same environment

[1]the aero-drag of the hull and crew is modeled in a conservative way. This simulations represent a worst case scenario on an under performing plant

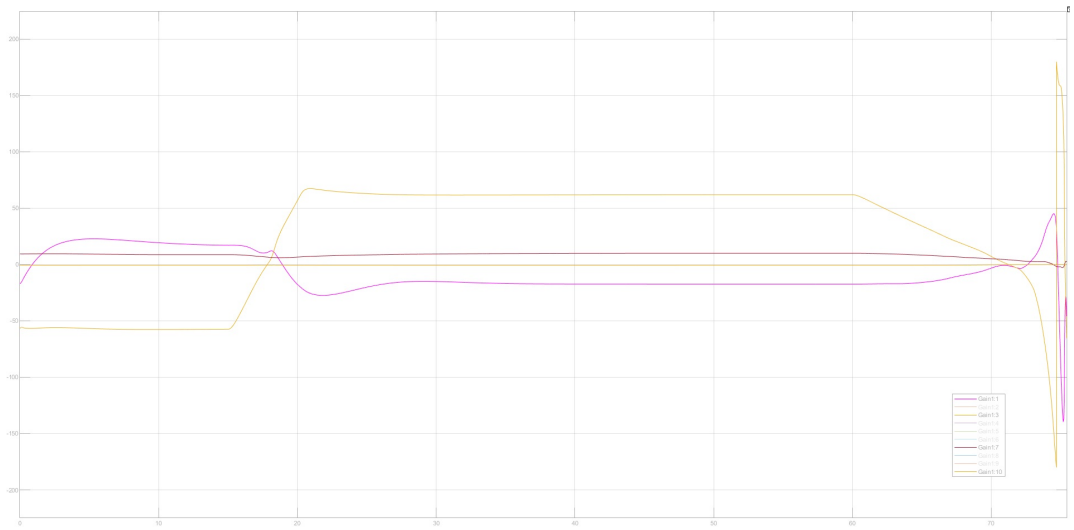

Figure 6.6: Well performed tack followed by a slower one

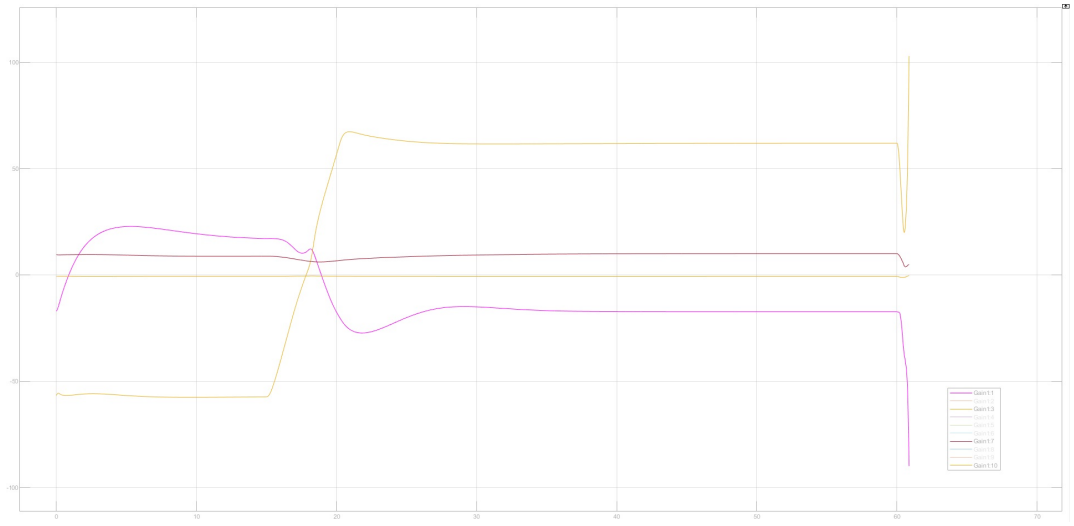

Figure 6.7: Well performed tack followed by a faster one

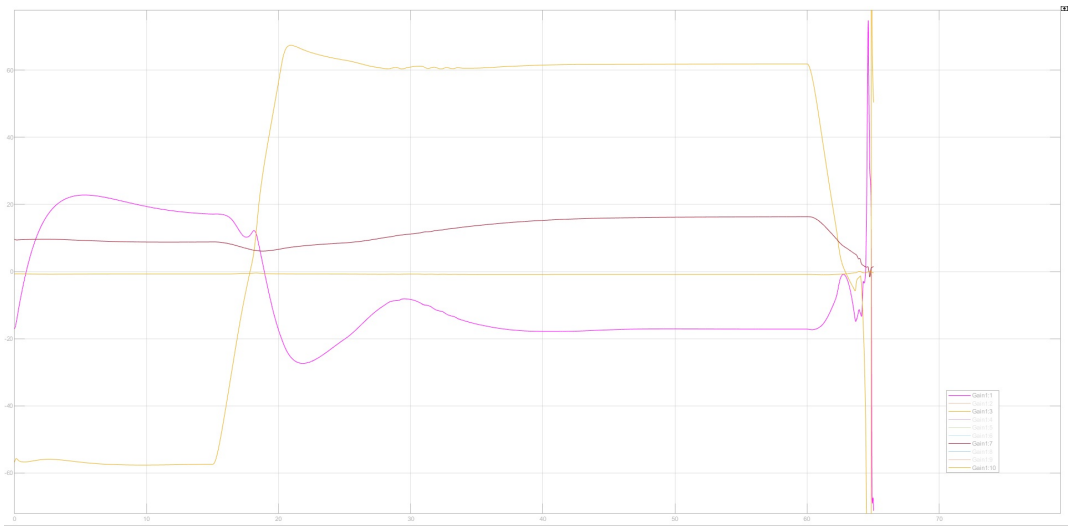

Figure 6.8: Two identical tacks performed in different TWS

Reducing the windage of the boat will result in a critical improvement of its performance both in straight line/VMG performance and maneuverability during tacks. The same consideration cannot be applied on jibes, since in this kind of maneuvers the actual dead zone spreads in a narrower range of TWA and, even while running dead (TWA$\simeq \pm 180°$), the drag experienced by the boat is proportional to ($(V_{b_x} - TWS)^2$. Given the boat speeds at which jibes occur, we can assume an AW of a light breeze coming from the bow with less intense aero-drag effects, therefore, we don't have the necessity of a fast rotation. Thus, we can always perform a jibe in high wind. The reduction in $\phi_{[ref]}$, given by the Eq: 5.3 in broad reach sailing, coupled with the Eq:5.2 Y_{crew} reduction actually increases the VMG performance. As a matter of fact, on fast boats the apparent wind decreases when sailing "deep" and the sail force that it can produce is low. Righting the boat on this condition reduces the actual dead zone of the jibe.

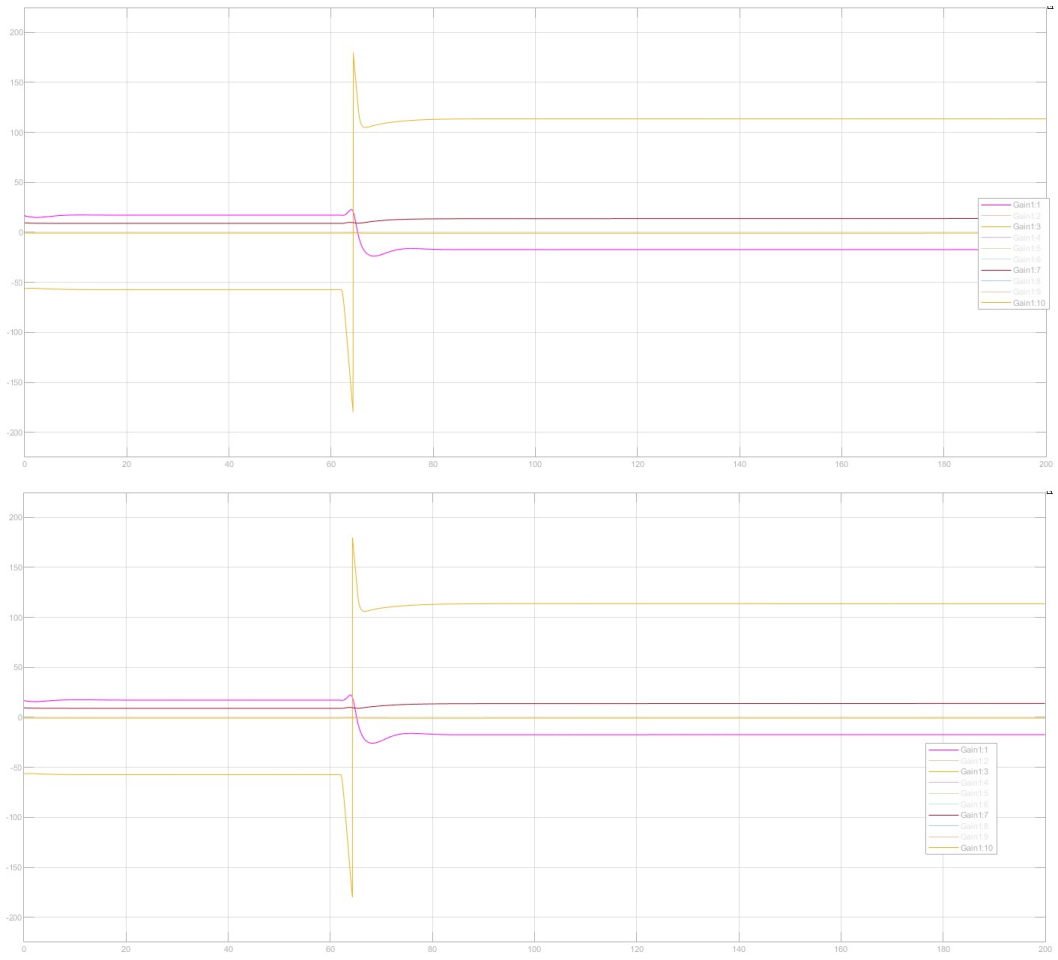

Figure 6.9: Two well performed Jibes

we will perform similar tack simulation, but this time we will include rough seas (Wave height 0.6m)to compare the performance between the two integrator architectures. The reduced integral architecture had to perform the second maneuver, in increased TWS, faster to complete it stably, showing worst performance during rough sea state tack, with the adjoint consideration that the already mentioned intermittent oscillation arising in the complete integrator feedback pales when compared to the oscillation induced by waves.

A remark has to be made on the fact that all tack simulations have to be performed in Forced fast mode, since the boat experiences a huge loss in speed due to high drag and no thrust inside the dead angle. While the "standard" mode read the speed loss and tried to overcome it by increasing the AoA$_s ail$, which inside such range of TWA only produces more drag and lateral forces destabilizing the maneuver, with the forced fast mode the boat sailed smoothly trough the dead zone and arrived at the new tack with minor effort, because the tendency of the boat to always accelerate is constant and accepted by the platform throughout the maneuver.

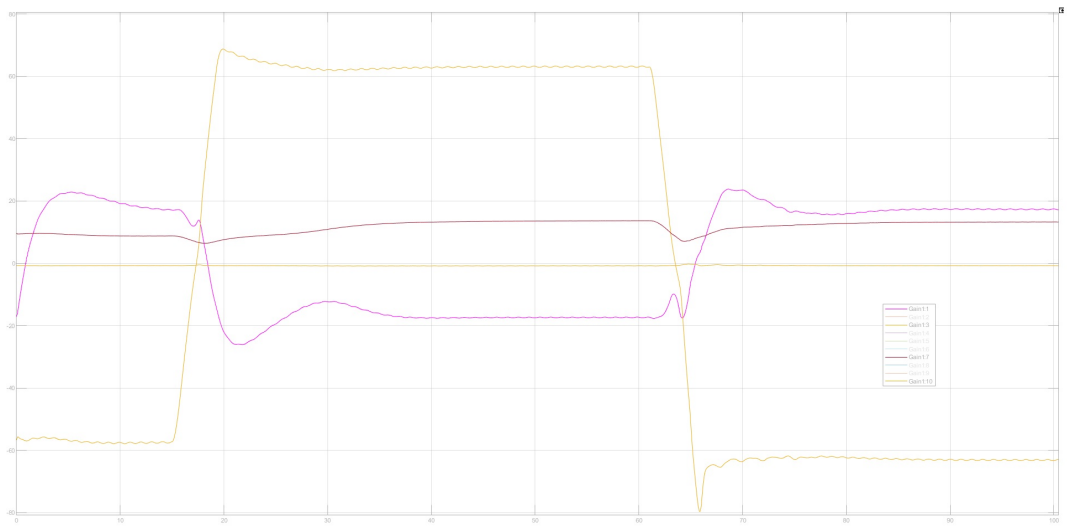

Figure 6.10: Two tacks in 0.2m wave in "Forced Fast" mode

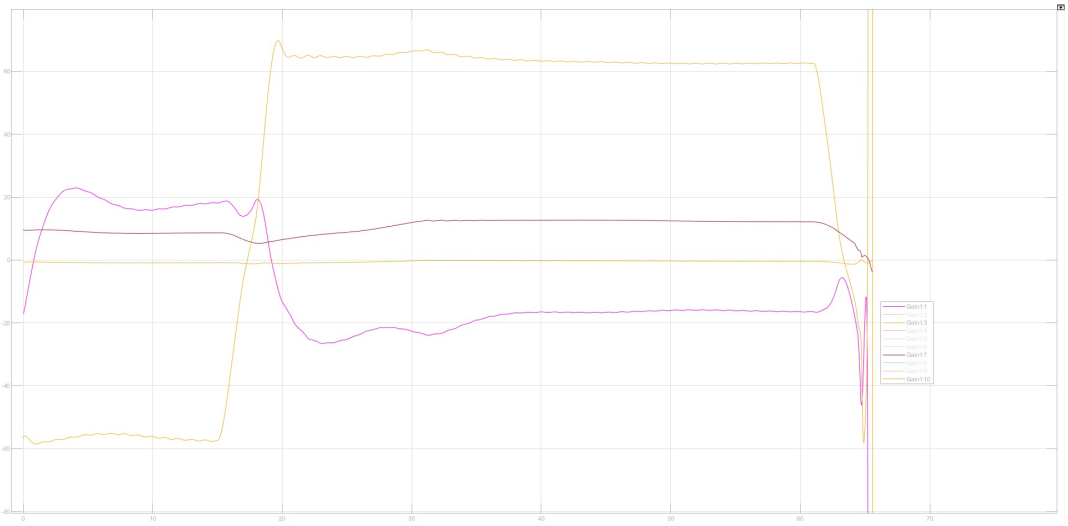

Figure 6.11: Two tacks in 0.2m wave in "Standard" mode

To underline the different behavior of forced fast and standard mode we can take a closer look at the boat speed in the last maneuver. As we can see in the time period within the two tacks, the boat experiences an enormous increase of forward speed due to the increased true wind (4m/s $\rightarrow$ 8m/s), but if we zoom in on the velocity we can see that the forced fast mode experiences 13.6 m/s of top speed which is 1m/s faster than the speed obtained in standard mode. On top of that, we can clearly see that the tendency of the standard mode is to slow down, while the preferable forced fast configuration carries its top speed up until the new maneuver is initiated. Being the main limitation of the boat the slowest speed experienced during maneuvers, where we may end up stalling the foils and splashing into the water, initiating the maneuver at a greater speed allows us to carry more speed during the turns, widening the narrow margin in which we are 12.5 ms max speed std decreasing

6.3 Sensitivity

To check the stability for parameters variations, we performed a Monte Carlo simulation with 300 instances, varying geometrical data, sailing points and environmental condition. The same instances were performed with both the reduced integral feedback loop and the complete one always in fast forced mode. To address the results, we focussed on simulation time (simulated), knowing that the simulation is automatically interrupted when the boat experiences relevant instability ($\phi \geq 70°$) or experience ventilation [2] Further indication of instability can be addressed by observing the ϕ angle variance which is supposed to be stable troghtout the whole simulation time. For sake of completeness, in each simulation the boat experiences a gust (both in angle and wind speed) at t=35s and a bear away to a variable TWS at t= 80s to cover as many situations as possible in a single run. To totally define the sea state we fixed the wave length to 100m that, coupled with the initial speed of 9.5m/s, gives a wave period of 10.5s

Paramater	Minimum value	Maximum Value
Wave Height	0 m	1m
TWS	4 m/s	7 m/s
x_{crew}	-0.6 m	0.6 m
Main-foil Incidence	-5°	5°
Gust rotation Angle	-11.5°	11.5°
Gust speed variation	-1 m/s	5 m/s
Bear Away HDG	57°	137°

Table 6.1: Different weights

[2] once the tip of a strut is airborne it experience an intense, unrecoverable vertical force (downward) applied on its centroid allowing us to detect the unlucky event through the same parameterϕ

It has to be noticed that the bear away is performed in a fixed amount of time (10s) therefore larger bear aways imply a faster rotation of the $\psi_{[ref]}$ during the simulation.

$$\phi_{[ref]} = \begin{cases} \phi_0 & \text{if } t \leq t_m \\ \phi_0(1 - 0.1(t - t_m)) + \phi_{BA_{HDG}}(0.1(t - t_m)) & \text{if } t_m \leq t \leq t_m + 10s \\ \phi_{BA_{HDG}} & \text{if } t \geq t_m + 10s \end{cases} \tag{6.1}$$

Since the highest rotation experienced in any circumstance in this Monte Carlo simulation is $8^{\circ/s}$ we can assume that an eventual instability arise from sources different from the rotation alone. The results of the Monte Carlo simulation, especially for the reduced architecture, show that in a high wave environment the sensitivity to parameters variations is increased, while the results in the complete integral feedback loop are somehow more scattered along the wave variation axis, implying another source of instability.

6.3.1 Reduced Integral Iesults

The sea state by itself, although necessary, having the whole set of unstable simulations between 0.77 and 1m of wave height, is not sufficient to destabilize the boat. There are in fact, many instances where the boat completed all the simulation's tasks even in a high sea state up to 0.99m of wave height. We experienced 3 instances, all of which terminated in less than 9 seconds where the the wave height was around 1m. We can trace back the instability to the instantaneous vertical component of the local water velocity at t=0 but there are not other similarities in parameter active at that time:

- Main foil incidence +0.3 0 -0.3°
- TWS 4.9 5.8 6.1m/s
- X_c 0.00 0.04 0.25m

The specific time at which the interruptions occur ($3/4\pi$) can indicate a ventilation event. A possible alternative explanation (not proven) could be numerical instability.

We also notice 3 instances that concluded the simulation around t=50s Those instabilities, still on rough sea state (0.93÷0.98 m), can be traced to the positive angular gust (header 9.1÷10.3°) where the reduced thrust will reduce the capability of overcoming waves' crests. The other common parameter was the backward position of the crew X_c=-0.1÷-0.4. For instance a similar parameter combination with the crew weight shifted forward only failed at the bear away t=80s (new $TWA_{[ref]}$=135°).

The bear away maneuver collected 34 fails all in a sea state *geq* 0.77m with a slight unbalance to the high gust intensity and positive angular wind rotations (lift). Knowing the physics of sailboat, it is easy to imagine that the combined action of the gust (speed and angle)on the already the oscillatory motion given by the sea state can destabilize enough the platform to fail the rotation triggered by the TWA change.

6.3.2 Complete Integral Results

The complete integral architecture performed quite poorly when compared with the reduced one, its instability is spread all around with 1 fail at t=4s, 22 fail related to gusts and 38 fails related to the bear away. The first source of sensibility through the gust (but still not sufficient alone) is related to a forward X_c position since all but two of the simulation that experienced instability had the crew positioned between 0.25m and 0.6m in front of the boat origin. The two outsiders had bad luck and waves above 0.97m. The 38 fails at the last check point suffered a combination of rough sea state and fast rotational rates during the bear away. On average the simulation that failed at the maneuver stage kept going for more time (up to 13s more)

6.3.3 Comparison

It has to be noticed that any parameters combination experienced by the Complete architecture, within Monte Carlo simulation, has been simulated on the reduced architecture too. Therefore, a direct comparison can be made. The reduced feedback loop achieve greater stability and robustness, and should be chosen over its counterpart to be implemented in an hypothetical autonomous vehicle. As already mentioned, the integration of the strictly minimum number of parameters needed for a stable flight greatly improve the feedback loop performance. The reduced Integral error keeps the unavoidable variables on spot, while allowing some tracking drift on other parameters. The fewer variables taken into account allow the feedback loop to have a much more precise behavior tailored to the platform specific dynamics greatly reducing sensitivity.

6.4 Performance Tricks: how to exploit physics to increase performance

on marginally flyable condition (TWS$\lessapprox$ 2.5 ms) the reduced integral feedback loop performs better than the complete one, which develops unhealthy oscillation faster resulting in a degraded performance of the boat.

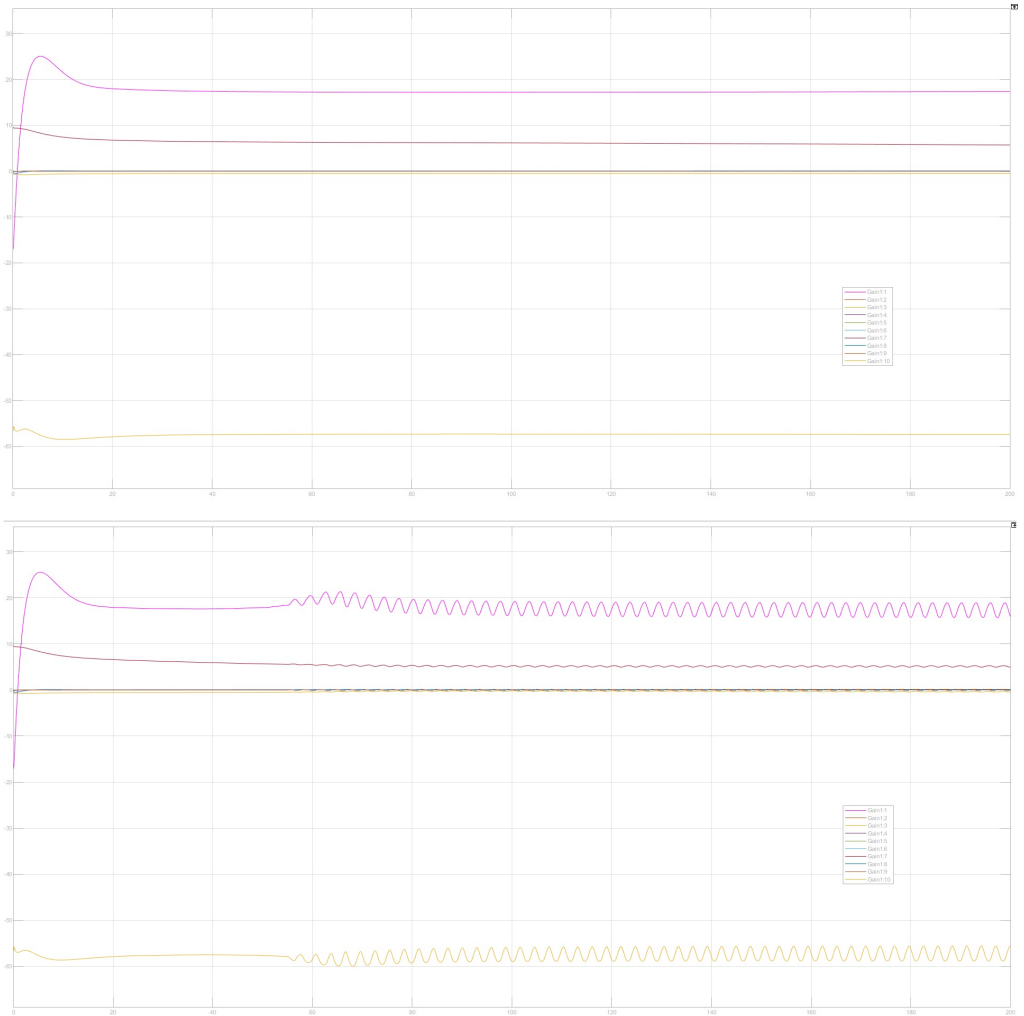

Figure 6.12: Flight in marginally conditions

As many experienced sailors can affirm, especially in low wind condition the boat can experience a speed hysteresis that impacts on the performance. Since the vessel sails in the apparent wind, a fast boat can "produces" its own wind. To verify that the model experiences the same condition we executed two simulations at TWS=2.5. In the first one we performed a little bear away followed by a luff of the same magnitude, and we ended up at a boat speed of 6.11 m/s. By switching the order of luff and bearing away in the same identical condition, we completed the simulation at a lower speed of 5.5 m/s. This foreseen difference in speed is due to the fact that the boat bearing away experiences a broader TWA, thus AWA that increases thrust and consequently the boat speed, thus the AWS. With the increased wind felt by the boat, we expect a greater force produced by the sail. After the luff, the increased wind is carried through the maneuver, allowing the boat speed to stabilize around a greater value with respect to the simulation where the luff is performed earlier. This example is just a hint on the non linearity generated by the sail/wind interaction.

Another performance gain, whose completion can only be performed while actively sailing the model through a joystick, is the exploitation of potential energy during tacks in marginally TWS condition. The tack is performed after a little bear away to carry more speed trough the maneuver. On top of that, before initiating the tack the flight height is increased up to the ventilation limit, the spare altitude allows the boat to glide down while sailing in the dead zone conserving speed. Once the wind comes from the new side, the rotation is continued to an angle greater than the desired one allowing a stronger acceleration in the new tack[3]. Once the boat speed is greater than the starting, one we can head up to the desired heading.

[3]unfortunately the English language does not distinguish between tack (maneuver) and tack (side of sailing point with respect to the wind direction)

Conclusion

In This Master Thesis project we have modeled a promising Foiling sailboat layout and tested many different control loop architectures to achieve stable flight and stable maneuvering in a variety of different environmental conditions. We used as a reference a boat design developed for the 1001Vela Challenge and compliant with R3 Regulation. The design arises from a feasibility study and, where parameters were not certain, the worst case scenario was applied. Despite this, the emerging performances were outstanding for a sail vehicle, even with hampered model parameters. Through an extensive use of the MATLAB/Simulink suite, we found viable trim conditions later used as starting points for the various simulations. We have proposed multiple feedback loop architectures on different variables and, after an extensive work of closed loop performance evaluations, we selected two architectures. One falls into the classical LQ OCP theory and the other was dictated by necessity. They both ended up to be promising for a practical implementation. The latter showed great robustness over geometrical and environmental parameter variation, and can be suggested for further studying with the aim of a practical implementation. We addressed the maneuvering with a linear gain scheduler achieving good results. Nevertheless, a deeper study of a more complex maneuvering scheduler could, in theory, increase the envelope in which smooth tack transitions can be achieved. Moreover, the addition of an AI based trajectory planner for jibes and especially tack maneuvers can further expand environmental variables range in which maneuvers can smoothly be performed

The complexity of the task, the multitude of variables comprised in this problem, and the design intrinsic great energetic efficiency for long range applications lead to the belief that the autonomous foiling boat subject is far from exhausted and is prone to further extensive studying in the near future.

Bibliography

[1] C.Casarosa *Meccanica del volo*. Pisa University Press.

[2] G.Buresti *Elements of Fluid Dynamics.* Imperial College Press

[3] Newman, John Nicholas (1977). *Marine hydrodynamics.* Cambridge, Massachusetts: MIT Press.

[4] M.Francioni A.Liverani *Feasibility study of an hydro-foiling dinghy with R3 class compliance*. UNIBO internal report 2019.

[5] Stevens, Brian, and Frank Lewis. *Aircraft Control and Simulation*, 2nd ed. Hoboken, NJ: John Wiley & Sons, 2003.

[6] Zipfel, Peter H. *Modeling and Simulation of Aerospace Vehicle Dynamics*. 2nd ed. Reston, VA: AIAA Education Series, 2007.

[7] Thor I. Fossen. *Handbook of Marine Craft Hydrodynamics and Motion Control* John Wiley & Sons 2011

[8] Fabio Fossati *Aero-Hydrodynamics and the Performance of Sailing Yachts: The Science Behind Sailboats and Their Design* International Marine/Ragged Mountain Press January 1

[9] A.V. Johansson S.Wallin *An Introduction to Turbulence* KTH

[10] *http://www.tspeer.com/Wingmasts/teardropPaper.htm*

[11] *https://web.archive.org/web/20160827051053/http://foils.org/ONeill_Hyd_L*

[12] *http://www.1001velacup.eu/regolamento/regolamento-di-classe.html*

[13] *http://www.oneoceankayaks.com/kayakpro/kayakgrid.htm*